Article:
Aad, G., Aakvaag, E., Abbott, B. et al. (2886 more authors) (2025) Search for charged Higgs bosons produced in top-quark decays or in association with top quarks and decaying via H±→τ±ντ in 13 TeV pp collisions with the ATLAS detector. Physical Review D, 111 (7). 072006. ISSN 2470-0010

https://doi.org/10.1103/physrevd.111.072006

Search for charged Higgs bosons produced in top-quark decays or in association with top quarks and decaying via $H^{\pm} \to \tau^{\pm}\nu_{\tau}$ in 13 TeV pp collisions with the ATLAS detector

G. Aad *et al.*[*]
(ATLAS Collaboration)

(Received 10 January 2025; accepted 18 February 2025; published 9 April 2025)

Charged Higgs bosons produced either in top-quark decays or in association with a top quark, subsequently decaying via $H^{\pm} \to \tau^{\pm}\nu_{\tau}$, are searched for in 140 fb^{-1} of proton-proton collision data at $\sqrt{s} = 13$ TeV recorded with the ATLAS detector. Depending on whether the top quark is produced together with the $H^{\pm}$ decays hadronically or semileptonically, the search targets τ + jets or τ + lepton final states, in both cases with a τ-lepton decaying into a neutrino and hadrons. No significant excess over the Standard Model background expectation is observed. For the mass range of $80 \leq m_{H^{\pm}} \leq 3000$ GeV, upper limits at 95% confidence level are set on the production cross section of the charged Higgs boson times the branching fraction $\mathcal{B}(H^{\pm} \to \tau^{\pm}\nu_{\tau})$ in the range 4.5 pb–0.4 fb. In the mass range 80–160 GeV, assuming the Standard Model cross section for $t\bar{t}$ production, this corresponds to upper limits between 0.27% and 0.02% on $\mathcal{B}(t \to bH^{\pm}) \times \mathcal{B}(H^{\pm} \to \tau^{\pm}\nu_{\tau})$.

DOI: 10.1103/PhysRevD.111.072006

I. INTRODUCTION

The discovery of a new boson at the Large Hadron Collider (LHC) [1] in 2012 [2,3], with a measured mass close to 125 GeV [4–6], opens the question of whether this particle could be part of an extended scalar sector. Charged Higgs bosons[1] are predicted in several extensions of the Standard Model (SM) that add a second doublet [7,8] or triplets [9–12] to its scalar sector. For H^+ masses below the top-quark mass ($m_{H^+} < m_{\text{top}}$), the main production mechanism is through the decay of a top quark, $t \to bH^+$, in double-resonant top-quark production ($t\bar{t}$). In this mass range, the decay $H^+ \to \tau\nu$ usually dominates in a two-Higgs-doublet model (2HDM) type-II, although $H^+ \to cs$ and cb may also become sizable at low ratio of the vacuum expectation values of the two Higgs doublets, $\tan\beta$. For H^+ masses above the top-quark mass ($m_{H^+} > m_{\text{top}}$), the leading production mode is $gg \to tbH^+$ (single-resonant top-quark production) [13]. For the heavy H^+, the $H^+ \to tb$ channel is dominant, but since the coupling of H^+ to leptons is proportional to $\tan\beta$, the branching fraction $H^+ \to \tau\nu$ remains sizable for large values of $\tan\beta$. In the intermediate-mass region ($m_{H^+} \simeq m_{\text{top}}$) the H^+ production occurs via the double-resonant, single-resonant and top-quark exchange production processes, along with their interference [14]. Figure 1 illustrates the main production modes for charged Higgs bosons in proton-proton (pp) collisions.

There are many earlier searches for charged Higgs bosons at colliders. The Large Electron–Positron Collider (LEP) experiments excluded the H^+ mass below 80 GeV at 95% confidence level (CL), considering only the decays $H^+ \to cs$ and $H^+ \to \tau\nu$ under the assumption $\mathcal{B}(H^+ \to cs) + \mathcal{B}(H^+ \to \tau\nu) = 1$ [15]. The ATLAS and CMS Collaborations searched for charged Higgs bosons in Run 1 with pp collisions at $\sqrt{s} = 7$–8 TeV probing the mass range below the top-quark mass with the $\tau\nu$ [16–20], cb [21] and cs [22,23] decay modes, as well as the mass range above the top-quark mass with the $\tau\nu$, tb, WZ decay modes [18,20,24,25]. Both experiments also performed searches with Run 2 pp collisions at $\sqrt{s} = 13$ TeV in the $\tau\nu$ [26,27], tb [28,29], WZ [30,31], HW [32,33], cb [34] and cs [35,36] decay channels. The intermediate mass region was probed for the first time in the search for $H^+ \to \tau\nu$ [26,27].

No evidence of charged Higgs bosons was found in any of these searches. The ATLAS and CMS experiments also searched for neutral scalar resonances decaying to a τ-lepton pair [37,38], sensitive to the habemus Minimal Supersymmetric Standard Model (hMSSM) [39,40] in some regions of its parameter space. A recent Run 2 $H^+ \to cb$

[*]Full author list given at the end of the article.

[1]In the following, charged Higgs bosons are denoted H^+, with the charge-conjugate H^- always implied. Generic symbols are also used for particles produced in association with charged Higgs bosons and in their decays.

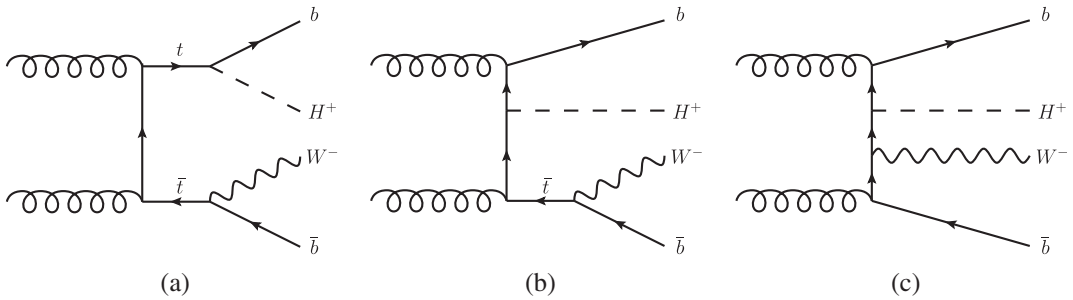

FIG. 1. Examples of leading-order Feynman diagrams contributing to the production of charged Higgs bosons in pp collisions: (a) double-resonant top-quark production that dominates at low H^+ masses, (b) single-resonant top-quark production that dominates at large H^+ masses, (c) top-quark exchange production. The interference between these three main diagrams becomes most relevant in the intermediate-mass region.

analysis by the ATLAS Collaboration [34] observed an excess above the SM background with a global significance of 2.5σ at the 130 GeV H^+ mass hypothesis. This result, coupled with the tension in semi-leptonic B-meson decays from the combination of measurements at several flavor experiments [41], support the viability of the 2HDM which can accommodate flavor changing neutral currents [42,43]. Therefore, further investigation into the decays of the charged Higgs boson is well motivated [44].

This publication describes a search for charged Higgs bosons in the mass range 80–3000 GeV, produced either in top-quark decays or in association with a top quark, decaying via $H^+ \to \tau\nu$, with a subsequent decay of the τ-lepton into a neutrino and hadrons (referred to as τ_{had}). Depending on the decay mode of the W boson originating from the top quark produced together with the H^+, two channels are targeted: τ_{had} + jets if the W boson decays into a $q\bar{q}'$ pair, or τ_{had} + lepton if the W boson decays into an electron or muon and at least one neutrino (directly or via a leptonically decaying τ lepton). The search is optimized for a generic 2HDM type-II scenario [8] and results are presented as 95% CL upper limits on cross section times branching fraction for the H^+ production and decay to the $\tau\nu$ final state. Interpretations are performed in the context of the hMSSM and the M_h^{125} scenario of the Minimal Supersymmetric Standard Model (MSSM) where all superpartners are chosen to be heavy [45].

This analysis uses the full Run 2 dataset of pp collisions at $\sqrt{s} = 13$ TeV collected with the ATLAS experiment at the LHC, corresponding to 140 fb^{-1}, and thus it supersedes the result of an earlier search based on the partial Run 2 dataset [26]. With respect to the previous analysis, the mass range of the search is expanded (previously 90–2500 GeV), the identification of τ_{had} candidates benefits from a new approach based on recurrent neural networks providing better signal purity, and the data-driven estimation of background from misidentified τ_{had} candidates is upgraded. Additionally, the modeling of the efficiency of the missing transverse energy trigger in simulation, as well as the modeling of $t\bar{t}$ and W + jets backgrounds is improved. The final signal-to-background discriminating variable is changed from a boosted decision tree [46] to a mass parametrized neural network (PNN) [47], similar to e.g. the H^+ search in the tb channel presented in Ref. [28]. These improvements result in an increased sensitivity to a hypothetical H^+ signal by up to a factor of two (four) in the low (high) mass region compared to the previous ATLAS search [26].

II. ATLAS DETECTOR

The ATLAS experiment [48] at the LHC is a multipurpose particle detector with a forward-backward symmetric cylindrical geometry and a near 4π coverage in solid angle.[2] It consists of an inner tracking detector surrounded by a thin superconducting solenoid providing a 2 T axial magnetic field, electromagnetic and hadronic calorimeters, and a muon spectrometer. The inner tracking detector covers the pseudorapidity range $|\eta| < 2.5$. It consists of silicon pixel, silicon microstrip, and transition radiation tracking detectors. Lead/liquid-argon (LAr) sampling calorimeters provide electromagnetic (EM) energy measurements with high granularity within the region $|\eta| < 3.2$. A steel/scintillator-tile hadronic calorimeter covers the central pseudorapidity range ($|\eta| < 1.7$). The end cap and forward regions are instrumented with LAr calorimeters for EM and hadronic energy measurements up to $|\eta| = 4.9$. The muon spectrometer surrounds the calorimeters and is based on three large superconducting air-core toroidal magnets with eight coils each. The field integral of the toroids ranges

[2]ATLAS uses a right-handed coordinate system with its origin at the nominal interaction point (IP) in the center of the detector and the z-axis along the beam pipe. The x-axis points from the IP to the center of the LHC ring, and the y-axis points upwards. Polar coordinates (r, ϕ) are used in the transverse plane, ϕ being the azimuthal angle around the z-axis. The pseudorapidity is defined in terms of the polar angle θ as $\eta = -\ln\tan(\theta/2)$ and is equal to the rapidity $y = \frac{1}{2}\ln(\frac{E+p_z}{E-p_z})$ in the relativistic limit. Angular distance is measured in units of $\Delta R \equiv \sqrt{(\Delta y)^2 + (\Delta\phi)^2}$.

TABLE I. List of SM background processes, generators utilized for matrix-element (ME) calculations, parton shower and hadronization, the PDF sets used, the cross section to which the total expected event yield is normalized, and the order to which the background processes were calculated. All background cross sections are normalized to NNLO predictions, except for diboson events, where the NLO prediction is used.

Background process	Generator and parton shower	PDF	Cross section [pb]	ME order
$t\bar{t}$	POWHEG-BOX v2 [58] and Pythia 8 [59]	NNPDF3.0NLO [60]	832	NLO
Single top quark t channel	POWHEG-BOX v2 and Pythia 8	NNPDF3.0NLO	217	NLO
Single top quark s channel			10.3	NLO
Single top quark Wt channel			72	NLO
$W(\ell\nu)+$ jets	Sherpa 2.2.1 [61]	NNPDF3.0NNLO	2.0×10^4	NNLO
$Z/\gamma^*(\ell\ell,\nu\nu)+$ jets	Sherpa 2.2.1	NNPDF3.0NNLO	2.1×10^3	NNLO
WW	POWHEG-BOX v2 and Pythia 8	CT10NLO [62]	55	NLO
WZ			26	NLO
ZZ			8.4	NLO

between 2.0 and 6.0 T m across most of the detector. The muon spectrometer includes a system of precision tracking chambers up to $|\eta|=2.7$ and fast detectors for triggering up to $|\eta|=2.4$. The luminosity is measured mainly by the LUCID-2 [49] detector, which is located close to the beampipe. A two-level trigger system is used to select events [50]. The first-level trigger is implemented in hardware and uses a subset of the detector information to accept events at a rate below 100 kHz. This is followed by a software-based trigger that reduces the accepted event rate to 1 kHz on average depending on the data-taking conditions. A software suite [51] is used in data simulation, in the reconstruction and analysis of real and simulated data, in detector operations, and in the trigger and data acquisition systems of the experiment.

III. DATA AND SIMULATED EVENT SAMPLES

The dataset used in this analysis, collected during stable beam conditions and with all ATLAS subsystems fully operational, corresponds to an integrated luminosity of 140 fb^{-1} of pp collisions at $\sqrt{s}=13$ TeV collected during 2015–2018 [52].

The simulated Monte Carlo (MC) samples used are based on the ATLAS full Geant4 simulation [53,54] and are reconstructed using the same analysis chain as the data. SM background samples include $t\bar{t}$ and single-top-quark production, W and Z plus jets with leptonic vector boson decays and diboson production. All samples are scaled by k factors so that the estimated background yields correspond to the recent theoretical predictions on the cross sections at next-to-next-to-leading order (NNLO) or next-to-leading order (NLO). Finally, all MC events are overlaid with additional minimum-bias events generated with Pythia v8.186 [55] using the A3 set of tuned parameters [56] and the NNPDF2.3LO [57] set of parton distributions functions (PDF) to simulate the effect of multiple pp collisions per bunch crossing (pileup), at a variable rate. The simulated events are then weighted to match the pileup distribution observed in data. The full list of simulated SM backgrounds is presented in Table I.

Simulated events of H^+ signal are generated in three distinct mass regions using the narrow-width approximation with MadGraph5_aMC@NLO [63] at either leading order (LO) or NLO in QCD using the respective NNPDF3.0 set. The choice of renormalization and factorization scale settings is motivated by Refs. [13,14].

(1) In the low mass region ($m_{H^+}<140$ GeV), $t\bar{t}$ events with a subsequent decay of one top quark to a H^+ and a bottom quark are generated using LO calculations only. The type-II 2HDM model is used and dynamic renormalization and factorization QCD scales are chosen ($\mu_R=\mu_F=H_T/2=1/2\sum_i\sqrt{m_i^2+p_{Ti}^2}$, where the sum goes over all final state partons from the hard scatter). The contribution from $t\bar{t}$ events with both top quarks decaying to bH^+ and single-top-quark events with a subsequent $t\to bH^+$ decay is negligible.

(2) In the intermediate mass region (140 GeV $\leq m_{H^+}<200$ GeV), nonresonant, single- and double-resonant top-quark processes with a W boson, a H^+ and two bottom quarks in the final state are generated in the four-flavor scheme (4FS)[3] at LO. The type-II 2HDM model with static QCD scales ($\mu_R=\mu_F=125$ GeV) is used.

(3) In the high mass region ($m_{H^+}\geq200$ GeV), H^+ production in association with a single top quark is generated in the 4FS at NLO. The type-II 2HDM model is used and the dynamic QCD scales are chosen ($\mu_R=\mu_F=H_T/3=1/3\sum_i\sqrt{m_i^2+p_{Ti}^2}$).

[3]In the matrix-element calculation, only gluons and first- and second-generation quarks are considered when defining the proton parton distribution functions.

For all signal samples, the parton-level generator is interfaced to Pythia 8 [59] with the NNPDF2.3LO PDF set and the A14 [64] set of tuned parameters.

IV. ANALYSIS

The general analysis strategy, objects definition, event selection as well as background and signal modeling follow those of Ref. [26].

A. Event reconstruction and selection

Recorded events are filtered by requiring at least one primary vertex [65] with two or more associated tracks with $p_{\mathrm{T}} > 400$ MeV, that they pass a good-quality requirement, and that all relevant detector components were in good operating condition [66].

Hadronic τ-lepton [67,68] decays are identified using a recurrent neural network (RNN) designed to discriminate against quark- and gluon-initiated jets [69]. In the following, reconstructed τ candidates, corresponding to the visible part of a hadronic τ-lepton decay (hereafter called $\tau_{\text{had-vis}}$), are required to have $p_{\mathrm{T}} > 20$ GeV, $|\eta| < 2.5$, excluding $1.37 < |\eta| < 1.52$, an electric charge of $+1$ or -1, and one or three associated tracks, also referred to as 1- or 3-prong, respectively. A separate boosted decision tree is used to reject electrons that are misidentified as 1-prong $\tau_{\text{had-vis}}$ candidates. Electrons and muons are reconstructed and identified as reported in Refs. [70,71], respectively. Jets are reconstructed using the particle flow approach [72] and clustered with the anti-k_t algorithm [73,74] with a radius parameter $R = 0.4$. Additionally, jets originating from the hadronization of bottom quarks are identified (b tagged) using advanced algorithms combined into the DL1r tagger as described in Ref. [75]. A working point corresponding to an average efficiency of 70% for b jets in simulated $t\bar{t}$ events is chosen. When several objects defined above overlap geometrically, an overlap removal procedure is applied as described in Ref. [26]. The missing transverse momentum in the event, with magnitude $E_{\mathrm{T}}^{\text{miss}}$, is determined from the reconstructed objects according to Ref. [76]. Simulated events are corrected for differences between data and MC simulation seen in b-tagging efficiencies and mistag rates as well as minor differences in electron (e), muon (μ) and $\tau_{\text{had-vis}}$ reconstruction, identification, and isolation efficiencies.

The analysis of the τ_{had} + jets channel is based on events accepted by $E_{\mathrm{T}}^{\text{miss}}$ triggers [77] with a threshold at 70, 80, 90 or 110 GeV, depending on the data-taking period.[4] Because the $E_{\mathrm{T}}^{\text{miss}}$ trigger is not accurately modeled in simulation, the efficiency of the trigger decision as a function of reconstructed $E_{\mathrm{T}}^{\text{miss}}$ is fitted using a Gaussian error function ($erf(x) = \frac{1}{\sqrt{2\pi\sigma^2}} \int_{-\infty}^{x} e^{-(t-\mu)^2/2\sigma^2} dt$) in both data and simulation, following a method similar to that in Ref. [78]. The ratio of the *erf* fit in data to that in simulation is then used to reweight the simulated events.

The τ_{had} + jets channel signal region (SR) further requires at least one *medium* $\tau_{\text{had-vis}}$ candidate, corresponding to 75% (60%) efficiency for 1-prong (3-prong) $\tau_{\text{had-vis}}$ candidates [68], with $p_{\mathrm{T}} > 40$ GeV and $|\eta| < 2.3$, no *loose* leptons (electron [70] or muon [71]) with $p_{\mathrm{T}} > 20$ GeV, at least three jets with $p_{\mathrm{T}} > 25$ GeV, of which at least one is b tagged, $E_{\mathrm{T}}^{\text{miss}} > 150$ GeV and $m_{\mathrm{T}} > 50$ GeV.[5] A signal-depleted control region (CR) is defined for the τ_{had} + jets channel (τ_{had} + jets $t\bar{t}$ CR), to probe the modeling of the $t\bar{t}$ background. The $t\bar{t}$-enriched τ_{had} + jets $t\bar{t}$ CR has the same event selection as described above, except $m_{\mathrm{T}} > 50$ GeV is replaced with $m_{\mathrm{T}} < 100$ GeV and at least two b jets are required. The purity of this region in top-quark backgrounds, i.e. $t\bar{t}$ and single-top-quark events is around 90%. To ensure full orthogonality, events satisfying the τ_{had} + jets $t\bar{t}$ CR selection criteria are excluded from the τ_{had} + jets SR.

The τ_{had} + lepton channel, made of the τ_{had} + electron and τ_{had} + muon subchannels, is based on events accepted by single-lepton triggers. Triggers for electrons or muons [79–81] with low E_{T} or p_{T} thresholds respectively (20–26 GeV depending on the data-taking period) and isolation requirements are combined in a logical OR with triggers having higher p_{T} thresholds (60–120 GeV for electrons, 50 GeV for muons) and looser isolation or identification requirements to maximize the efficiency.

The τ_{had} + lepton channel SR events are selected requiring exactly one *tight* lepton (electron [70] or muon [71]) with $p_{\mathrm{T}} > 30$ GeV and $|\eta| < 2.5$ ($|\eta| < 2.47$, excluding $1.37 < |\eta| < 1.52$) for muons (electrons) matched to the single-lepton trigger object, exactly one *medium* $\tau_{\text{had-vis}}$ candidate with $p_{\mathrm{T}} > 30$ GeV, $|\eta| < 2.3$ and an electric charge opposite to that of the lepton, at least one b-tagged jet with $p_{\mathrm{T}} > 25$ GeV and $E_{\mathrm{T}}^{\text{miss}} > 50$ GeV. Additionally, a $t\bar{t}$-enriched CR is defined for the τ_{had} + lepton channel (τ_{had} + lepton $t\bar{t}$ CR), to derive $t\bar{t}$ modeling corrections in this channel. This CR has the same event selection as described above, with the addition of $E_{\mathrm{T}}^{\text{miss}} > 80$ GeV, $m_{\mathrm{T}} < 70$ GeV and at least two b-tagged jets. This CR selection is a subset of τ_{had} + lepton selection described above. To maintain orthogonality of the regions, events satisfying the τ_{had} + lepton $t\bar{t}$ selection are rejected from the τ_{had} + lepton SR.

Two further signal-depleted CRs are defined for the τ_{had} + lepton channel. The $\tau_{\text{had}} + e/\mu$ b-veto CR relies on the same event selection as the SR, vetoing any b-tagged

[4] Due to differing pile-up conditions which impact the trigger rates.

[5] m_{T}, the transverse mass of the highest-p_{T} $\tau_{\text{had-vis}}$ candidate and $E_{\mathrm{T}}^{\text{miss}}$ is defined as $m_{\mathrm{T}}(\tau_{\text{had-vis}}, E_{\mathrm{T}}^{\text{miss}}) = \sqrt{2 p_{\mathrm{T}}^{\tau} E_{\mathrm{T}}^{\text{miss}} (1 - \cos\Delta\phi_{\tau,\text{miss}})}$, where $\Delta\phi_{\tau,\text{miss}}$ is the azimuthal angle between the $\tau_{\text{had-vis}}$ candidate and the direction of the missing transverse momentum.

TABLE II. Summary of requirements for the regions used in the analysis. When applicable, units are in GeV, τ refers to $\tau_{\text{had-vis}}$ in the cut definitions, and j refers to jets in the region names. FF MJ and FF $W+j$ denote multijet and $W+$ jets CRs, respectively, defined to determine $\tau_{\text{had-vis}}$ fake factors as described in Sec. IV B.

Cut	SR $\tau+j$	$t\bar{t}(\tau j)$	$W+j$	FF MJ	FF $W+j$	SR $\tau+\ell$	$t\bar{t}(\tau\ell)$	b veto	$e+\mu$
$p_{\text{T}}(\tau)$	>40	>40	>40	>30	>30	>30	>30	>30	⋯
N_{ℓ}	0	0	0	0	1	1	1	1	2
$p_{\text{T}}(\ell)$	⋯	⋯	⋯	⋯	>30	>30	>30	>30	>30
$q(\tau)\times q(\ell)$	⋯	⋯	⋯	⋯	⋯	-1	-1	-1	⋯
N_{jet}	≥ 3	≥ 3	≥ 3	≥ 3	⋯	≥ 1	≥ 2	≥ 1	≥ 1
$p_{\text{T}}(\text{lead}-\text{jet})$	>25	⋯	>25	>25	⋯	>25	>25	>25	>25
$N_{b\text{-jet}}$	≥ 1	≥ 2	0	0	0	≥ 1	≥ 2	0	≥ 1
$E_{\text{T}}^{\text{miss}}$	>150	>150	>150	<80	⋯	>50	>80	>50	>50
$m_T(\tau, E_{\text{T}}^{\text{miss}})$	>50	<100	<100	>50	⋯	⋯	<70	⋯	⋯
Other	[a]				[b]	[a]			[c]

[a]Note that the SRs reject events in the overlap with the corresponding $t\bar{t}$ regions.
[b]There is an additional requirement that 60 GeV $< m_T(e, E_{\text{T}}^{\text{miss}}) <$ 160 GeV.
[c]The two ℓs must be an oppositely charged $e+\mu$ pair.

jets. This region is enriched in $W+$ jets events with true e/μ and a jet misidentified as $\tau_{\text{had-vis}}$ and $Z+$ jets events with Z boson decaying to a pair of τ leptons. The $t\bar{t}$ enriched CR ($e+\mu b$-tag CR) uses SR event selection, except that a *tight* (and oppositely charged) $e+\mu$ pair is required instead of a $\tau_{\text{had-vis}}+$ lepton pair. This CR has a very high purity ($>99.8\%$) of top-quark background events.

Control regions are used to validate the agreement between data and background simulation or derive necessary corrections, but are not included in the final likelihood fit. A summary of the selection applied to the regions used in this analysis is shown in Table II.

B. Background modeling

Background modeling relies on simulated MC events for SM backgrounds containing the $\tau_{\text{had-vis}}$ object matched to a true hadronic τ-lepton decay at the generator level or containing electrons or muons reconstructed and identified as $\tau_{\text{had-vis}}$ objects ($\ell \to \tau_{\text{had}}^{\text{fake}}$).

Events that contain quark- or gluon-initiated jets and no true τ_{had} can enter the SR when one of these jets is reconstructed and misidentified as a $\tau_{\text{had-vis}}$ candidate (fake $\tau_{\text{had-vis}}$). A data-driven fake-factor (FF) method is used to estimate this background. The ratios of the number of events with fake $\tau_{\text{had-vis}}$ objects satisfying the $\tau_{\text{had-vis}}$ identification criteria ($N_{\text{CR fake}}^{\tau\text{-ID}}$) to the number of events with fake anti-$\tau_{\text{had-vis}}$ objects satisfying the very loose requirement on the $\tau_{\text{had-vis}}$ identification but failing to meet the loose identification requirement ($N_{\text{CR fake}}^{\text{anti-}\tau\text{-ID}}$) [68] are measured in the dedicated CRs. The fake factors ($\text{FF} = N_{\text{CR fake}}^{\tau\text{-ID}}/N_{\text{CR fake}}^{\text{anti-}\tau\text{-ID}}$) are determined in bins of $\tau_{\text{had-vis}}$ p_{T}, separately for 1-prong and 3-prong candidates. To estimate the number of background events with fake $\tau_{\text{had-vis}}$ in the SR, the measured FFs are applied to the number of events with fake anti-$\tau_{\text{had-vis}}$ objects obtained by requiring the SR selection, but replacing the $\tau_{\text{had-vis}}$ with the anti-$\tau_{\text{had-vis}}$ selection criteria ($N_{\text{SR fake}}^{\tau} = N_{\text{SR fake}}^{\text{anti-}\tau\text{-ID}} \times \text{FF}$). The number of events with a fake $\tau_{\text{had-vis}}$ candidate in each region is obtained by subtracting the number of simulated events containing a true τ_{had} or $\ell \to \tau_{\text{had}}^{\text{fakes}}$ from the number of data events ($N_{\text{fake}}^{\tau} = N_{\text{data}}^{\tau} - N_{\text{MC true}}^{\tau} - N_{\text{MC}}^{\ell\to\tau}$).

Two CRs with different fractions of quark- and gluon-initiated jets are used to determine the FFs. The FF multijet CR relies on multijet event triggers [82] and is defined by selecting events satisfying an offline selection similar to that of the $\tau_{\text{had}}+$ jets SR, but requiring $p_{\text{T}}(\tau) > 30$ GeV, $E_{\text{T}}^{\text{miss}} < 80$ GeV and vetoing any b-tagged jets. The FF $W+$ jets CR is defined by selecting events passing an offline selection similar to that of the $\tau_{\text{had}}+$ lepton SR, but requiring 60 GeV $< m_{\text{T}}(\ell, E_{\text{T}}^{\text{miss}}) <$ 160 GeV and vetoing b-tagged jets. In the FF multijet CR, the contamination arising from correctly reconstructed and identified $\tau_{\text{had-vis}}$ objects is small (8%), while in the FF $W+$ jets CR, this contamination is about 20%. In the corresponding anti-τ-ID regions, the fraction of events with a true τ_{had} is negligible in the FF multijet CR and is around 6% in the FF $W+$ jets CR. The contribution from true τ_{had} events in the above mentioned categories is estimated using simulation and is subtracted from the number of observed events in each region. The FF multijet CR contains similar fractions of quark- and gluon-initiated jets, while the FF $W+$ jets CR is dominated by quark-initiated jets. The SR is expected to have contributions from both types, but with different fractions. In order to estimate the fraction of gluon-initiated jets in the signal region, a template-fit method in the anti-τ-ID region is used, based on a discriminating variable that is sensitive to the source of the jet. This fraction is used to estimate combined fake factors, which are linear combinations of the fake factors measured in the multijet and $W+$ jets CRs. The variable chosen for the templates is

the $\tau_{\text{had-vis}}$ width defined as $w_\tau = \frac{\sum [p_{\text{T}}^{\text{track}} \times \Delta R(\tau_{\text{had-vis}}, \text{track})]}{\sum p_{\text{T}}^{\text{track}}}$ for tracks satisfying $\Delta R(\tau_{\text{had-vis}}, \text{track}) < 0.4$.

Due to inaccurate data modeling at high jet multiplicities arising in the $t\bar{t}$ and $W+\text{jets}$ simulations, data-based corrections are applied to the MC prediction, following the example of Refs. [28,34]. Reweighting factors, $R(x)$, are derived by comparing the MC prediction to the data in dedicated CRs, separately for $t\bar{t}$ and $W+\text{jets}$ MC samples. For the $\tau_{\text{had}}+\text{lepton}$ channel, $R(x)$ is determined in the $\tau_{\text{had}}+\text{lepton}$ $t\bar{t}$ CR as a function of $m_{\text{eff}} = \sum_{\text{jets}} p_{\text{T}}^{\text{jets}} + p_{\text{T}}^{\tau} + p_{\text{T}}^{\text{lepton}} + E_{\text{T}}^{\text{miss}}$ and for the $\tau_{\text{had}}+\text{jets}$ channel in the $\tau_{\text{had}}+\text{jets}$ $t\bar{t}$ CR as a function of $m_{\text{eff}} = \sum_{\text{jets}} p_{\text{T}}^{\text{jets}} + p_{\text{T}}^{\tau} + E_{\text{T}}^{\text{miss}}$. Reweighting factors for the $W+\text{jets}$ sample are derived as a function of jet multiplicity in the $W+\text{jets}$ CR of the $\tau_{\text{had}}+\text{jets}$ channel and are applied to the simulated $W+\text{jets}$ events in both $\tau_{\text{had}}+\text{jets}$ and $\tau_{\text{had}}+\text{lepton}$ channels. The overall event normalization factor from applying the reweighting factors ranges from 0.86 to 0.95.

C. Multivariate discriminant

Following the event selections described in Sec. IV A, kinematic variables that differentiate between the signal and backgrounds are combined into a multivariate signal-to-background discriminant using PNNs. The PNN response is parametrized with the generator-level H^+ mass, $m_{\text{truth}}^{H^+}$, and defines classifiers for all probed H^+ mass hypotheses, with continuous sensitivity to masses between them. The PNN output score for a given H^+ mass hypothesis discriminates between that signal and the SM backgrounds, and is used as the final discriminating variable for the statistical analysis. The training of the PNNs is performed using the Keras [83] library with the TensorFlow [84] library as a backend. Two separate PNNs are defined and trained for the $\tau_{\text{had}}+\text{jets}$ and $\tau_{\text{had}}+\text{lepton}$ channels using all signal samples at the same time, taking the value of the H^+ mass as a parameter.[6] The k-fold training method [85] is used with $k = 5$ in order to increase the effective statistics of the training sample and to prevent overtraining.

The input variables used to train the PNNs for the $\tau_{\text{had}}+\text{jets}$ and $\tau_{\text{had}}+\text{lepton}$ channels are mostly the four-momentum components of the reconstructed final state objects and are listed in Table III. For events with more than one $\tau_{\text{had-vis}}$ candidate or more than one b-tagged jet, the highest-p_{T} object is passed as input to the PNN. When comparing the PNN response for data and for the background model in regions that do not contain a $\tau_{\text{had-vis}}$ or b jets, a default value of zero is used for the corresponding input variables. The $\Upsilon = 2(p_{\text{T}}^{\tau\text{-track}}/p_{\text{T}}^{\tau_{\text{had-vis}}}) - 1$ variable [86], where $p_{\text{T}}^{\tau\text{-track}}$ refers to the track associated with the $\tau_{\text{had-vis}}$, is sensitive to τ-lepton polarization and helps discriminate between the SM background processes, where the $\tau_{\text{had-vis}}$ object stems from a vector-boson decay and signal, where τ_{had} is a decay product of a scalar particle. This variable is defined only for 1-prong tau decays, hence included uniquely in the PNN variable for events with a selected 1-prong $\tau_{\text{had-vis}}$ object. Due to correlations with some input variables entering the RNN $\tau_{\text{had-vis}}$ identification, the Υ distribution significantly differs between $\tau_{\text{had-vis}}$ and anti-$\tau_{\text{had-vis}}$ candidates. In order to ensure proper modeling of this distribution, an inverse transform sampling (Smirnov transform) is performed on the Υ variable of anti-$\tau_{\text{had-vis}}$ candidates entering the fake-factor background estimation [26].

TABLE III. List of kinematic variables used as input to the PNN in the $\tau_{\text{had}}+\text{jets}$ and $\tau_{\text{had}}+\text{lepton}$ channels. Here, ℓ refers to the selected lepton (electron or muon), while jet-1, jet-2 and jet-3 refer to the leading, second-leading and third-leading jet ordered in p_{T}. The list of jets includes b-jets. The Υ variable is sensitive to the polarization of the τ-lepton and is only defined for 1-prong $\tau_{\text{had-vis}}$ candidates. Hence, the PNN training is performed separately for events with a selected 1- or 3-prong $\tau_{\text{had-vis}}$ candidate.

PNN input variable	$\tau_{\text{had}}+\text{jets}$	$\tau_{\text{had}}+\text{lepton}$
p_{T}^{τ}, η^{τ}, ϕ^{τ}, E^{τ}	✓	✓
p_{T}^{ℓ}, η^{ℓ}, ϕ^{ℓ}, E^{ℓ}		✓
$p_{\text{T}}^{b\text{-jet}}$, $\eta^{b\text{-jet}}$, $\phi^{b\text{-jet}}$, $E^{b\text{-jet}}$	✓	✓
$p_{\text{T}}^{\text{jet-1}}$, $\eta^{\text{jet-1}}$, $\phi^{\text{jet-1}}$, $E^{\text{jet-1}}$	✓	✓
$p_{\text{T}}^{\text{jet-2}}$, $\eta^{\text{jet-2}}$, $\phi^{\text{jet-2}}$	✓	
$p_{\text{T}}^{\text{jet-3}}$, $\eta^{\text{jet-3}}$, $\phi^{\text{jet-3}}$	✓	
$p_{\text{T}}^{\text{jet-2}}$		✓
$E_{\text{T}}^{\text{miss}}$, $\phi^{E_{\text{T}}^{\text{miss}}}$	✓	✓
Υ (1-prong $\tau_{\text{had-vis}}$ only)	✓	✓
$m_{\text{truth}}^{H^+}$	✓	✓

The modeling of the PNN input variables as well as the output score is validated in the CRs. The PNN score in the $t\bar{t}$ enriched $\tau_{\text{had}}+\text{jets}$ $t\bar{t}$ CR, and the $W/Z+\text{jets}$ enriched b-veto CR of the $\tau_{\text{had}}+\mu$ channel are shown in Fig. 2 for an example H^+ mass of 170 GeV. The PNN score distributions for two example signal masses (170 GeV and 1000 GeV) are shown in Fig. 3 for the $\tau_{\text{had}}+\text{jets}$ SR and in Fig. 4 for the $\tau_{\text{had}}+\text{lepton}$ SRs.

D. Systematic uncertainties

Detector-related systematic uncertainties arise from the simulation of the electron and muon triggers, from electron and muon isolation criteria, from the reconstruction and identification of leptons, $\tau_{\text{had-vis}}$ objects and b jets, from the energy/momentum scale and resolution of all detector

[6] In the training process, samples for all H^+ mass hypotheses are normalized to the weighted number of background events. Background events enter the training multiple times, such that each event is assigned to every H^+ mass hypothesis once.

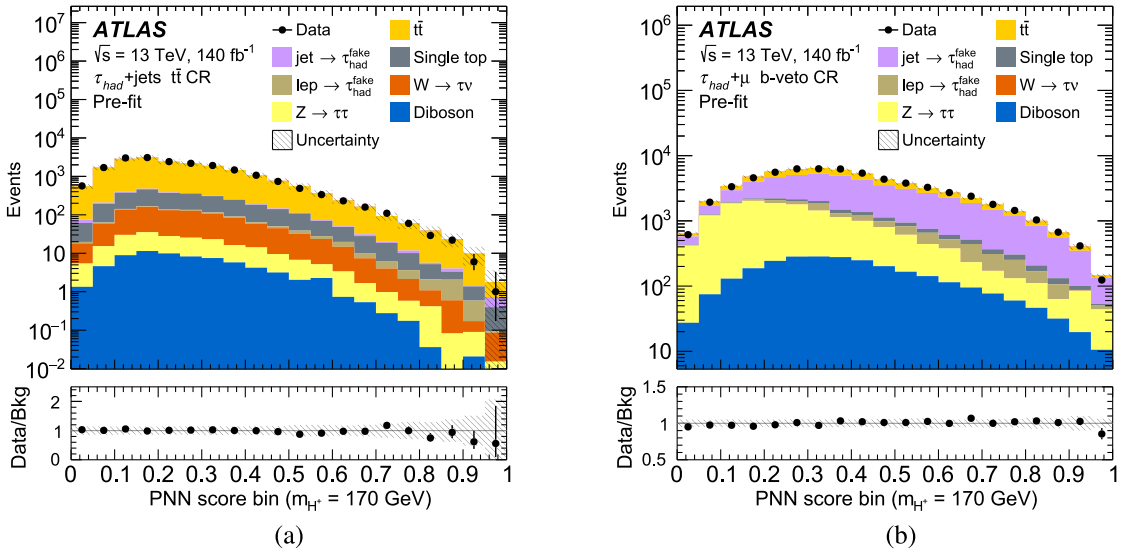

FIG. 2. Predicted and measured PNN score distributions before the fit to data ("Pre-fit") in (a) the $t\bar{t}$ enriched CR of the τ_{had} + jets channel and (b) the b-veto CR of the τ_{had} + muon channel enriched in the W/Z + jets events with jets faking $\tau_{\text{had-vis}}$, for the 170 GeV m_{H^+} hypothesis. The lower panel of each plot shows the ratio of data to the SM background prediction. The uncertainty bands include all statistical and systematic uncertainties. The bin boundaries of these distributions are spaced equally at intervals of 0.05 and do not represent the binning scheme used in the final fits.

objects, as well as from the reconstruction of the event $E_{\text{T}}^{\text{miss}}$. To assess the impact of most detector-related systematic uncertainties on the four-momenta of the analysis objects, the selection criteria are reapplied after varying a particular parameter by its ± 1 standard deviation value. These are complemented by variations of the scale factors related to efficiencies of physics objects reconstruction and identification. All detector-related systematic uncertainties are also propagated to the analysis objects used in the $E_{\text{T}}^{\text{miss}}$ calculation, and an additional uncertainty on its soft term is considered [76]. The effect of each systematic uncertainty, with the exception of those that demonstrate less than 0.5% deviation from the nominal value in all bins of the final discriminating variable as defined in Sec. V, is parametrized and included in the definition of the likelihood function used to statistically infer the final results.

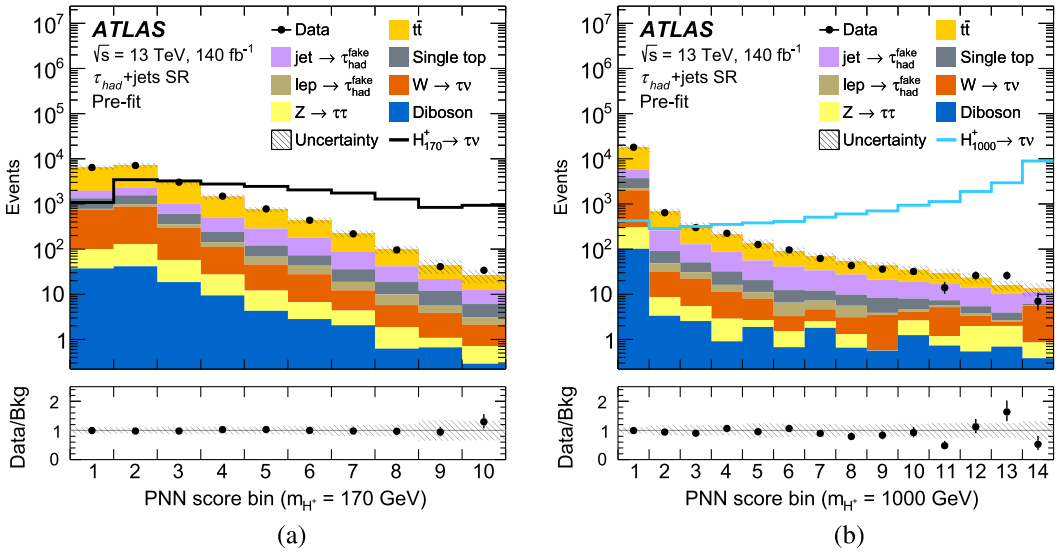

FIG. 3. PNN score distributions before the fit to data ("Pre-fit") in the SR of the τ_{had} + jets for the (a) 170 GeV and (b) 1000 GeV m_{H^+} hypotheses. The lower panel of each plot shows the ratio of data to the SM background prediction. The uncertainty bands include all statistical and systematic uncertainties. Bin boundaries are optimized for the best sensitivity of the final fit (see Sec. V) but are displayed as equidistant for better readability. Also shown are the expected signal distributions normalized to the total background yield.

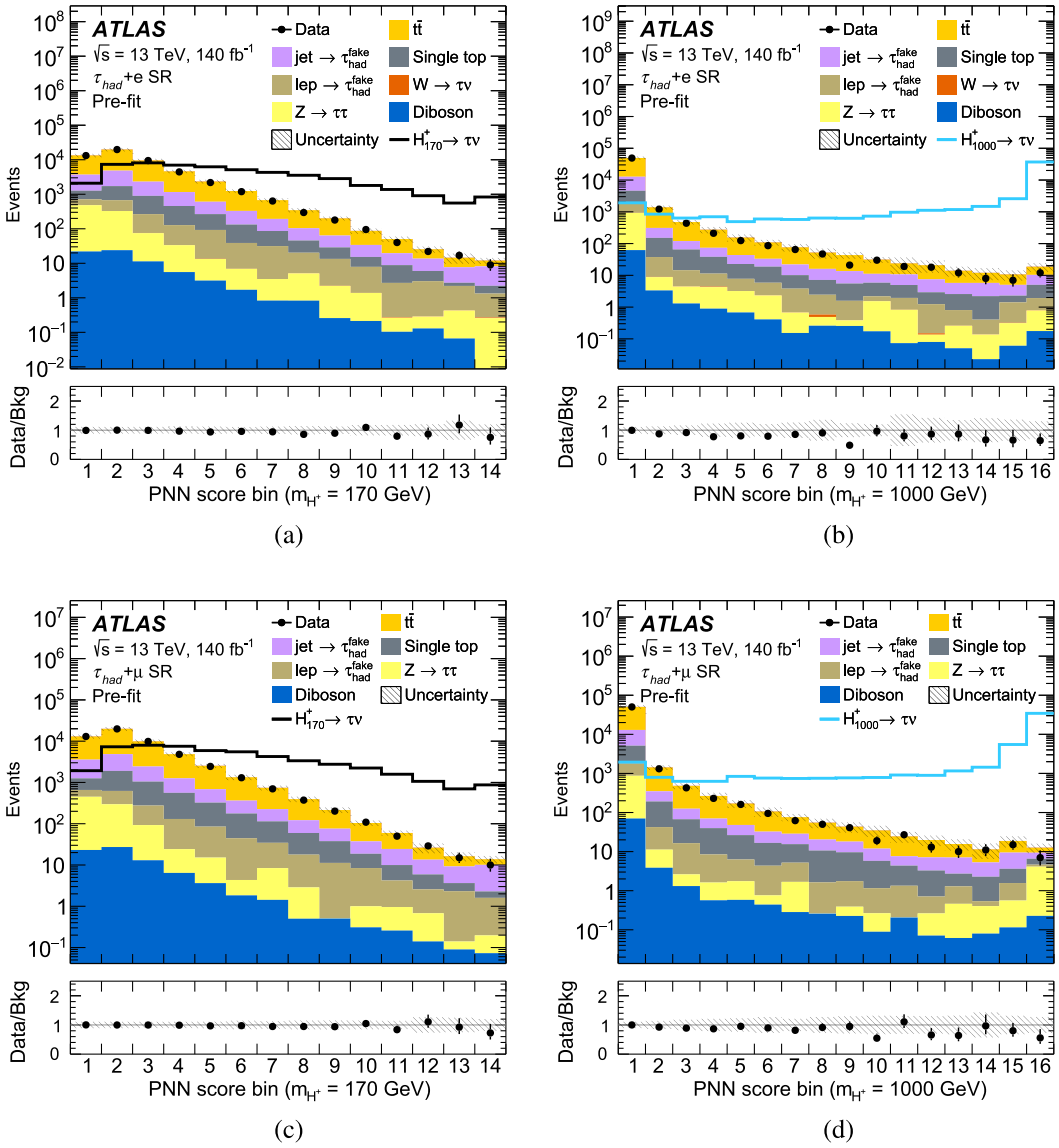

FIG. 4. PNN score distributions before the fit to data ("Pre-fit") in the SR of the τ_{had} + electron sub-channel for the (a) 170 GeV and (b) 1000 GeV m_{H^+} hypotheses and τ_{had} + muon subchannel for the (c) 170 GeV and (d) 1000 GeV m_{H^+} hypotheses. The lower panel of each plot shows the ratio of data to the SM background prediction. The uncertainty bands include all statistical and systematic uncertainties. Bin boundaries are optimized for the best sensitivity of the final fit (see Sec. V) but are displayed as equidistant for better readability. Also shown are the expected signal distributions normalized to the total background yield.

In the τ_{had} + jets channel, additional uncertainties are attributed to the evaluation of the trigger efficiency scale factors. These include (a) the effect of varying the selection criteria used for measuring the trigger efficiency, such as changing the number of required jets and b jets and applying different working points for the $\tau_{\text{had-vis}}$ and electron identification algorithms; (b) the impact of the fake $\tau_{\text{had-vis}}$ background modeling, which is assessed by measuring the trigger scale factors after subtracting the data-driven fake $\tau_{\text{had-vis}}$ estimate from the observed data and keeping only events with true $\tau_{\text{had-vis}}$ in simulation; and (c) statistical uncertainties in the values of the *erf* function parameters derived from the fit. The covariance matrix of the fitted parameters of the *erf* function is diagonalized and then propagated to the final fit as uncorrelated uncertainties.

Uncertainties in the estimation of background from quark- and gluon-initiated jets misidentified $\tau_{\text{had-vis}}$ objects arise from extraction of the FFs in the designated CRs as well as the determination of the combined FFs and application of those in the SRs. Uncertainties in the FFs include statistical uncertainty in the FF value estimated in each p_{T} bin of the CRs, a 5% uncertainty in the number of true τ_{had} objects in MC simulation which satisfy the $\tau_{\text{had-vis}}$ selection ($N^{\tau\text{-ID}}_{\text{MCtrue}}$) and a conservative 50% uncertainty in the number of these objects passing the anti-$\tau_{\text{had-vis}}$

selection ($N^{\text{anti-}\tau\text{-ID}}_{\text{MCtrue}}$). The former corresponds to the uncertainty in the $\tau_{\text{had-vis}}$ identification efficiency. There are no rigorous estimates of the latter, but the fractional contributions are small, as detailed in Sec. IV B. The Υ variable transform derived from the FF $W+\text{jets}$ CR is used as nominal while the one derived from the FF multijet CR is taken as a systematic uncertainty. The uncertainties in determining the combined FFs include the statistical uncertainty in the template fit to the $\tau_{\text{had-vis}}$ jet width as well as an uncertainty due to the p_{T} binning used for the template fit, which is estimated by varying the binning criteria. Furthermore, the CRs used to measure FFs are mostly dominated by light-quark (u, d, s) and gluon initiated jets reconstructed as $\tau_{\text{had-vis}}$, while in the SR with inverted $\tau_{\text{had-vis}}$ identification criteria, around 30%–40% of the reconstructed $\tau_{\text{had-vis}}$ candidates originate from heavy-flavor (HF) initiated jets. The larger width of HF jets compared to light jets leads to a bias in the template fit and consequently in the composition of the jets misidentified as $\tau_{\text{had-vis}}$ objects in the SRs. The bias is estimated in $t\bar{t}$ simulation by comparing the true yield of fake $\tau_{\text{had-vis}}$ to the one estimated using FFs and jet width templates from light jets alone obtained from simulation. The difference is used as an uncertainty on the fake $\tau_{\text{had-vis}}$ yield from the $t\bar{t}$ background. The largest single uncertainty on the fake $\tau_{\text{had-vis}}$ estimation comes from the HF jet contribution in the SR.

Systematic uncertainties associated with reweighting of $t\bar{t}$ and $W+\text{jets}$ MC samples include statistical uncertainties in the fitted values of the reweighting function parameters and the potential impact of signal contamination in CRs where reweighting factors are calculated. To estimate the number of signal events, the $m_{H^+}=90$ GeV cross section limit from Ref. [26] extrapolated[7] to $m_{H^+}=80$ GeV is used. The fractional contribution of the hypothetical signal amounts to 3.6% (3.8%) in the $\tau_{\text{had}}+\text{jets}$ ($\tau_{\text{had}}+\text{lepton}$) $t\bar{t}$ CRs and 0.5% in the $W+\text{jets}$ CR. An additional uncertainty associated with the extrapolation of the $t\bar{t}$ reweighting into the $\tau_{\text{had}}+\text{jets}$ ($\tau_{\text{had}}+\text{lepton}$) SR is estimated by using the reweighting functions obtained for the $\tau_{\text{had}}+\text{lepton}$ ($\tau_{\text{had}}+\text{jets}$) channel. In the case of the $W+\text{jets}$ background, a conservative 50% normalization uncertainty is considered.

Theoretical uncertainties on the main MC simulated backgrounds ($t\bar{t}$, single top quarks, $W+\text{jets}$) include contributions from renormalization and factorization scale variations, initial state radiation (ISR) and final state radiation (FSR), parton distribution functions, as well as parton shower and hadronization model. The latter is estimated using the difference between Pythia 8 (default) and Herwig7 [87] predictions, which is then symmetrized. The prescriptions used for ISR/FSR and scale variations are generator dependent, but typically involve varying the resummation damping factor up or down by a factor of two. For each variation, a dedicated reweighting of the $t\bar{t}$ and $W+\text{jets}$ MC samples is derived to avoid double counting of uncertainties.

Theoretical uncertainties on signal modeling include renormalization and factorization scale variations, PDF variations, as well as potential small acceptance loss due to the generator-level event selection used. The PDF and scale variations are additionally rescaled to maintain the nominal cross section.

The uncertainty in the integrated luminosity is 0.83% [88], obtained using the LUCID-2 detector [49] for the primary luminosity measurements, complemented by measurements using the inner detector and calorimeters. This uncertainty affects the normalization of all simulated samples.

V. RESULTS

The expected prefit number of events for all SM processes and the measured event yields in all three SRs are shown in Table IV. The contributions from hypothetical H^+ bosons are also listed, assuming a m_{H^+} hypothesis of 170 GeV or 1000 GeV, and with $\sigma(pp\to tbH^+)\times\mathcal{B}(H^+\to\tau\nu)$ set to 1 pb. The signal selection acceptance times efficiency for a m_{H^+} hypothesis of 170 GeV, as evaluated in an inclusive sample of simulated events where all possible τ-lepton and top-quark decays are considered, is 0.78%, 0.43% and 0.51% in the $\tau_{\text{had}}+\text{jets}$, $\tau_{\text{had}}+\text{electron}$ and $\tau_{\text{had}}+\text{muon}$ SR, respectively. These become 9.35%, 0.68% and 0.74% for $m_{H^+}=1000$ GeV. The large increase in the $\tau_{\text{had}}+\text{jets}$ SR comes from the $E^{\text{miss}}_{\text{T}}$ requirement, which becomes almost fully efficient for large m_{H^+}. The event yields measured in data are consistent with the SM background expectations in the three SRs.

The statistical interpretation is based on a simultaneous fit of the parameter of interest, i.e. $\mu\equiv\sigma(pp\to tbH^+)\times\mathcal{B}(H^+\to\tau\nu)$, and the nuisance parameters θ that encode statistical and systematic uncertainties, by means of a negative log-likelihood minimization. The combined binned likelihood function $\mathcal{L}(\mu,\theta)$ for the PNN score distributions is constructed as a product of Poisson probability terms over all bins in the three SRs ($\tau_{\text{had}}+\text{jets}$, $\tau_{\text{had}}+\text{electron}$ and $\tau_{\text{had}}+\text{muon}$). The binning of the discriminating variable is optimized to maximize the sensitivity of the analysis prior to looking at the data in the SRs.

The test statistic $\tilde{q}_\mu$ [89] used to test the compatibility of the data with the background-only and signal + background hypotheses is computed from the profile likelihood ratio. Upper limits on the signal production cross section times branching fraction are derived using a binned likelihood fit with the CL_S method [90]: for a given signal hypothesis, values of the production cross section times branching fraction $\sigma(pp\to tbH^+)\times\mathcal{B}(H^+\to\tau\nu)$

[7]Scaling by the ratio of the expected limits at 80 and 90 GeV.

TABLE IV. Prefit event yields for the backgrounds, hypothetical signal for two H^+ mass hypotheses, and the observed number of data events in each of the three SRs. The values shown for the signal assume $m_{H^+} = 170$ GeV and 1000 GeV, with a cross section times branching fraction $\sigma(pp \to tbH^+) \times \mathcal{B}(H^+ \to \tau\nu)$ corresponding to 1 pb. Combined statistical and systematic uncertainties are quoted.

	Event yields and uncertainties		
Sample	$\tau_{\text{had}} + \text{jets}$	$\tau_{\text{had}} + e$	$\tau_{\text{had}} + \mu$
True τ_{had}			
$t\bar{t}$	13400 ± 2000	39000 ± 6000	39000 ± 5000
Single top quark	1600 ± 400	2900 ± 400	3630 ± 330
$Z \to \tau\tau$	220 ± 110	900 ± 500	800 ± 400
$W \to \tau\nu$	1770 ± 270	2.4 ± 2.0	0.07 ± 0.21
Diboson (WW, WZ, ZZ)	120 ± 60	70 ± 35	80 ± 40
Misidentified jet $\to \tau_{\text{had-vis}}$	2430 ± 200	8500 ± 700	8200 ± 700
Misidentified $e, \mu \to \tau_{\text{had-vis}}$	280 ± 170	1000 ± 500	1000 ± 500
All backgrounds	19800 ± 2100	52000 ± 6000	53000 ± 6000
H^+ (170 GeV), $\sigma \times \mathcal{B} = 1$ pb	980 ± 150	580 ± 70	690 ± 80
H^+ (1000 GeV), $\sigma \times \mathcal{B} = 1$ pb	13000 ± 800	940 ± 60	1040 ± 70
Data	19650 ± 140	51500 ± 230	52730 ± 230

yielding $\text{CL}_S < 0.05$ are excluded at 95% CL. The asymptotic approximation [89] is used throughout the statistical analysis.

Figures 5 and 6 show the PNN score distributions corresponding to two example m_{H^+} hypotheses for the SRs of the $\tau_{\text{had}} + \text{jets}$ and $\tau_{\text{had}} + \text{lepton}$ channels, respectively. All plots are obtained after the statistical fitting procedure with the background-only hypothesis.

The data are found to be consistent under the background-only hypothesis. Exclusion upper limits are set at 95% CL on $\sigma(pp \to tbH^+) \times \mathcal{B}(H^+ \to \tau\nu)$ for the full mass range investigated, as well as on $\mathcal{B}(t \to bH^+) \times \mathcal{B}(H^+ \to \tau\nu)$ in the low H^+ mass range. Figure 7 shows the expected and observed combined exclusion limits as a function of m_{H^+}. The observed limits range from 4.5 pb to 0.4 fb. At low mass, the sensitivity of the analysis is driven

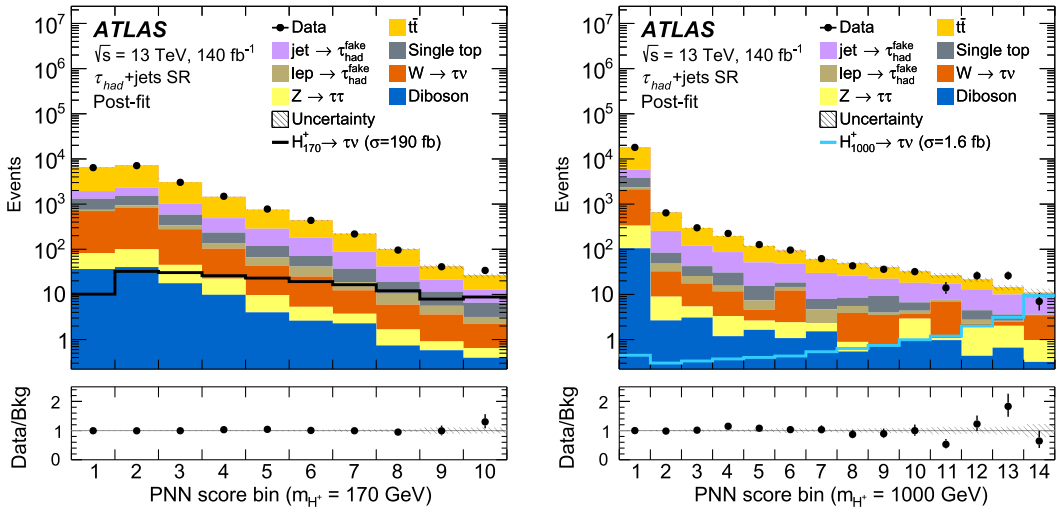

(a) (b)

FIG. 5. PNN score distributions after the fit to data ("Post-fit") under the background-only hypothesis in the SR of the $\tau_{\text{had}} + \text{jets}$ channel for the (a) 170 GeV and (b) 1000 GeV m_{H^+} hypotheses. The signal distribution of the 170 GeV (1000 GeV) H^+ mass hypothesis is shown by the solid black (teal) line, where the signal distribution is scaled to its expected 95% CL limit. The lower panel of each plot shows the ratio of data to the SM background prediction. The uncertainty bands include all statistical and systematic uncertainties. Bin boundaries are optimized for the best sensitivity of the final fit (see Sec. V) but are displayed as equidistant for better readability.

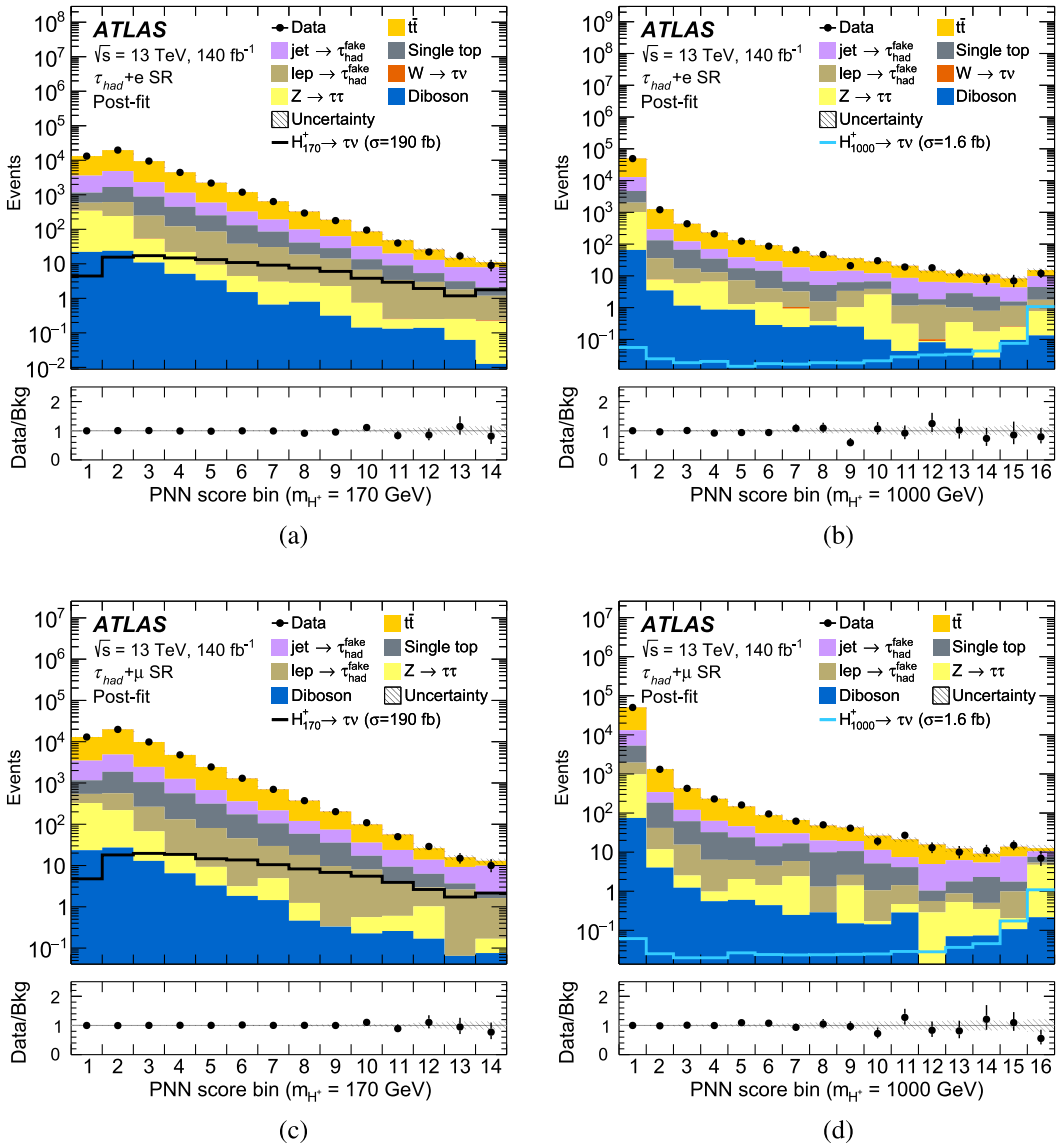

FIG. 6. PNN score distributions after the fit to data ("Post-fit") under the background-only hypothesis in the SR of the τ_{had} + electron subchannel for the (a) 170 GeV and (b) 1000 GeV m_{H^+} hypotheses and τ_{had} + muon subchannel for the (c) 170 GeV and (d) 1000 GeV m_{H^+} hypotheses. The signal distribution of the 170 GeV (1000 GeV) H^+ mass hypothesis is shown by the solid black (teal) line, where the signal distribution is scaled to its expected 95% CL limit. The lower panel of each plot shows the ratio of data to the SM background prediction. The uncertainty bands include all statistical and systematic uncertainties. Bin boundaries are optimized for the best sensitivity of the final fit (see Sec. V) but are displayed as equidistant for better readability.

by the τ_{had} + lepton channel, while at high mass the τ_{had} + jets channel dominates. For the mass range between 80 and 160 GeV, the limits on $\sigma(pp \to tbH^+) \times \mathcal{B}(H^+ \to \tau\nu)$ translate into observed limits between 0.27% and 0.02% on $\mathcal{B}(t \to bH^+) \times \mathcal{B}(H^+ \to \tau\nu)$ assuming the SM $t\bar{t}$ production cross section.

The impact from the various sources of systematic uncertainty is estimated by taking the difference in quadrature of the observed 1 sigma uncertainty ($\sigma(\hat{\mu})$) on the best fit μ value ($\hat{\mu}$) obtained when performing an unconditional signal-plus-background fit to observed data while considering all systematic uncertainties, to the $\sigma(\hat{\mu})$ obtained when performing a conditional fit with a certain set of systematic uncertainties fixed to their best fit values from the unconditional fit. The results for example m_{H^+} mass hypotheses 170 GeV and 1000 GeV are summarized in Table V.

Figure 8 shows the 95% CL exclusion limits on $\tan\beta$ as a function of m_{H^+} in the context of the hMSSM [91] and the M_h^{125} scenario of the MSSM [45]. The boundaries chosen correspond to regions in which theoretical predictions are available and in which this analysis has coverage. Exclusion limits for $m_{H^+} \leq 140$ GeV are not shown, as the hMSSM scenario is not valid in this range [40].

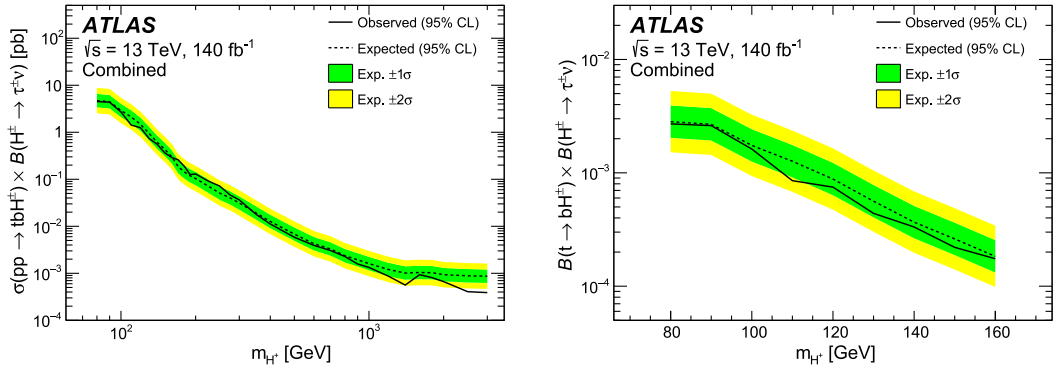

(a) (b)

FIG. 7. Observed and expected 95% CL exclusion limits on (a) $\sigma(pp \to tbH^+) \times \mathcal{B}(H^+ \to \tau\nu)$ and (b) $\mathcal{B}(t \to bH^+) \times \mathcal{B}(H^+ \to \tau\nu)$ as a function of m_{H^+}, from a combined fit in the $\tau_{\text{had-vis}}$ + jets and $\tau_{\text{had-vis}}$ + lepton channels. The surrounding shaded bands correspond to the 1σ and 2σ confidence intervals around the expected limit.

TABLE V. Impact from various sources of systematic uncertainty on $\sigma(\hat{\mu})$ (the observed 1σ uncertainty on $\hat{\mu}$) from the combined fit for two H^+ mass hypotheses: 170 GeV and 1000 GeV. The impact is obtained by taking the difference in quadrature of the uncertainty on $\hat{\mu}$ obtained when performing an unconditional signal + background fit to observed data [$\sigma(\hat{\mu}_{\text{ALL}})$], to the uncertainty on $\hat{\mu}$ obtained when performing a conditional fit with a certain set of systematic uncertainties fixed to their best fit values from the unconditional fit $\sigma(\hat{\mu}_{\text{group}})$. The impact is defined as, Impact $= \frac{\sqrt{|\sigma(\hat{\mu}_{\text{ALL}})|^2 - \sigma(\hat{\mu}_{\text{group}})^2} \times 100}{\sigma(\hat{\mu}_{\text{ALL}})}$. The row "Total" is obtained by computing the normalized difference in quadrature of the observed uncertainty from the unconditional fit, to a conditional fit where only statistical uncertainties are considered. In the absence of correlations and assuming Gaussian uncertainties, the row "Total" would be obtained by summing in quadrature the individual contributions of the systematic uncertainties.

Source of systematic uncertainty	Impact on $\sigma(\hat{\mu})$ [%]	
	$m_{H^+} = 170$ GeV	$m_{H^+} = 1000$ GeV
Experimental		
Luminosity	1.0	1.0
Trigger	12	4.1
$\tau_{\text{had-vis}}$	12	8.3
Jet	27	17
Electron	1.9	4.0
Muon	9.3	2.2
$E_{\text{T}}^{\text{miss}}$	35	3.3
Fake-factor method	21	16
Signal and background models		
$t\bar{t}$ modeling	20	14
Single-top-quark modeling	46	2.6
W/Z + jets modeling	13	51
Cross sections ($W/Z/VV/t$)	2.3	15
H^+ signal modeling	8.5	1.0
Total	84	70

At $\tan\beta = 60$, above which no reliable theoretical calculations exist, H^+ bosons with masses up to 1400 GeV are excluded, significantly improving on the limits reported in Ref. [26]. The hypothetical contribution from the H^+ decaying to tb with the subsequent tauonic top decay ($t \to b\tau^+\nu_\tau$) contributing to the low $\tan\beta$ region is small due to a low branching fraction of the semileptonic top-quark decay and has a lower reconstruction efficiency due to softer kinematics of the $\tau\nu$ system. Consequently, it is not considered in the derived exclusion, yielding a conservative result.

VI. CONCLUSIONS

A search for H^+ bosons produced either in top-quark decays or in association with top quarks, subsequently decaying via $H^+ \to \tau\nu$ is performed in the H^+ mass range 80–3000 GeV. Depending on whether the top quark produced together with the H^+ decays hadronically or semileptonically, the search targets τ + jets or τ + lepton final states, in both cases with a τ lepton decaying into a neutrino and hadrons. The dataset used for this analysis is from pp collisions at $\sqrt{s} = 13$ TeV, collected with the ATLAS detector at the LHC, and corresponds to an integrated luminosity of 140 fb^{-1}. The discrimination between signal and background is based on a neural network parametrized as a function of the H^+ mass.

The data are found to be in agreement with the Standard Model background expectation. Upper limits at 95% CL are set on the H^+ production cross section times branching fraction, $\sigma(pp \to tbH^+) \times \mathcal{B}(H^+ \to \tau\nu)$, ranging from 4.5 pb to 0.4 fb for H^+ masses in the range 80–3000 GeV. In the mass range 80–160 GeV, assuming the SM cross section for $t\bar{t}$ production, this corresponds to upper limits between 0.27% and 0.02% for the product of branching fractions $\mathcal{B}(t \to bH^+) \times \mathcal{B}(H^+ \to \tau\nu)$. The upper limits are interpreted in the hMSSM and, for the first time in the $\tau\nu$ final state, the M_h^{125} scenarios of the MSSM. This search contributes to the broad program of H^+ searches at

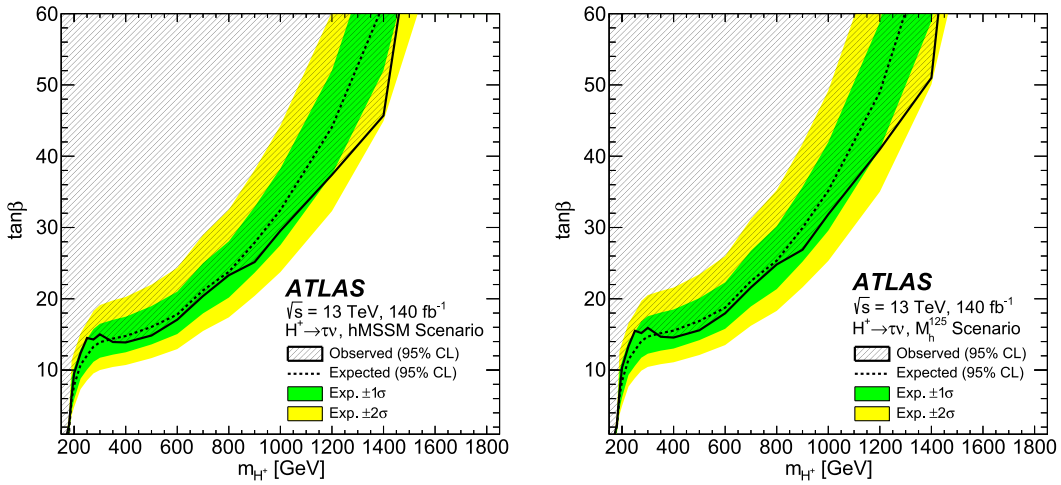

FIG. 8. Observed and expected 95% CL exclusion limits on $\tan\beta$ as a function of m_{H^+}, shown in the context of (a) the hMSSM and the (b) the M_h^{125} scenario of the MSSM, for $m_{H^+} > 150$ GeV and $(1 \leq \tan\beta \leq 60)$. The surrounding shaded bands correspond to the 1σ and 2σ confidence intervals around the expected limit.

the LHC and provides the most restrictive limits to date in this production and decay mode.

ACKNOWLEDGMENTS

We thank CERN for the very successful operation of the LHC and its injectors, as well as the support staff at CERN and at our institutions worldwide without whom ATLAS could not be operated efficiently. The crucial computing support from all WLCG partners is acknowledged gratefully, in particular from CERN, the ATLAS Tier-1 facilities at TRIUMF/SFU (Canada), NDGF (Denmark, Norway, Sweden), CC-IN2P3 (France), KIT/GridKA (Germany), INFN-CNAF (Italy), NL-T1 (Netherlands), PIC (Spain), RAL (UK) and BNL (USA), the Tier-2 facilities worldwide and large non-WLCG resource providers. Major contributors of computing resources are listed in Ref. [92]. We gratefully acknowledge the support of ANPCyT, Argentina; YerPhI, Armenia; ARC, Australia; BMWFW and FWF, Austria; ANAS, Azerbaijan; CNPq and FAPESP, Brazil; NSERC, NRC and CFI, Canada; CERN; ANID, Chile; CAS, MOST and NSFC, China; Minciencias, Colombia; MEYS CR, Czech Republic; DNRF and DNSRC, Denmark; IN2P3-CNRS and CEA-DRF/IRFU, France; SRNSFG, Georgia; BMBF, HGF and MPG, Germany; GSRI, Greece; RGC and Hong Kong SAR, China; ICHEP and Academy of Sciences and Humanities, Israel; INFN, Italy; MEXT and JSPS, Japan; CNRST, Morocco; NWO, Netherlands; RCN, Norway; MNiSW, Poland; FCT, Portugal; MNE/IFA, Romania; MSTDI, Serbia; MSSR, Slovakia; ARIS and MVZI, Slovenia; DSI/NRF, South Africa; MICIU/AEI, Spain; SRC and Wallenberg Foundation, Sweden; SERI, SNSF and Cantons of Bern and Geneva, Switzerland; NSTC, Taipei; TENMAK, Türkiye; STFC/UKRI, United Kingdom; DOE and NSF, USA. Individual groups and members have received support from BCKDF, CANARIE, CRC and DRAC, Canada; CERN-CZ, FORTE and PRIMUS, Czech Republic; COST, ERC, ERDF, Horizon 2020, ICSC-NextGenerationEU and Marie Skłodowska-Curie Actions, European Union; Investissements d'Avenir Labex, Investissements d'Avenir Idex and ANR, France; DFG and AvH Foundation, Germany; Herakleitos, Thales and Aristeia programmes co-financed by EU-ESF and the Greek NSRF, Greece; BSF-NSF and MINERVA, Israel; NCN and NAWA, Poland; La Caixa Banking Foundation, CERCA Programme Generalitat de Catalunya and PROMETEO and GenT Programmes Generalitat Valenciana, Spain; Göran Gustafssons Stiftelse, Sweden; The Royal Society and Leverhulme Trust, United Kingdom. In addition, individual members wish to acknowledge support from Armenia: Yerevan Physics Institute (FAPERJ); CERN: European Organization for Nuclear Research (CERN DOCT); Chile: Agencia Nacional de Investigación y Desarrollo (FONDECYT 1230812, FONDECYT 1230987, FONDECYT 1240864); China: Chinese Ministry of Science and Technology (MOST-2023YFA1605700, MOST-2023YFA1609300), National Natural Science Foundation of China (NSFC—12175119, NSFC 12275265, NSFC-12075060); Czech Republic: Czech Science Foundation (GACR—24-11373S), Ministry of Education Youth and Sports (FORTE CZ.02.01.01/00/22_008/0004632), PRIMUS Research Programme (PRIMUS/21/SCI/017); EU: H2020 European Research Council (ERC—101002463); European Union: European Research Council (ERC—948254, ERC 101089007, ERC,

BARD, 101116429), European Union, Future Artificial Intelligence Research (FAIR-NextGenerationEU PE00000013), Italian Center for High Performance Computing, Big Data and Quantum Computing (ICSC, NextGenerationEU); France: Agence Nationale de la Recherche (ANR-20-CE31-0013, ANR-21-CE31-0013, ANR-21-CE31-0022, ANR-22-EDIR-0002); Germany: Baden-Württemberg Stiftung (BW Stiftung-Postdoc Eliteprogramme), Deutsche Forschungsgemeinschaft (DFG—469666862, DFG—CR 312/5-2); Italy: Istituto Nazionale di Fisica Nucleare (ICSC, NextGenerationEU), Ministero dell'Università e della Ricerca (PRIN—20223N7F8K—PNRR M4.C2.1.1); Japan: Japan Society for the Promotion of Science (JSPS KAKENHI JP22H01227, JSPS KAKENHI JP22H04944, JSPS KAKENHI JP22KK0227, JSPS KAKENHI JP23KK0245); Netherlands: Netherlands Organisation for Scientific Research (NWO Veni 2020—VI.Veni.202.179); Norway: Research Council of Norway (RCN-314472); Poland: Ministry of Science and Higher Education (IDUB AGH, POB8, D4 no 9722), Polish National Agency for Academic Exchange (PPN/PPO/2020/1/00002/U/00001), Polish National Science Centre (NCN 2021/42/E/ST2/00350, NCN OPUS 2023/51/B/ST2/02507, NCN OPUS nr 2022/47/B/ST2/03059, NCN UMO-2019/34/E/ST2/00393, NCN and H2020 MSCA 945339, UMO-2020/37/B/ST2/01043, UMO-2021/40/C/ST2/00187, UMO-2022/47/O/ST2/00148, UMO-2023/49/B/ST2/04085, UMO-2023/51/B/ST2/00920); Slovenia: Slovenian Research Agency (ARIS Grant No. J1-3010); Spain: Generalitat Valenciana (Artemisa, FEDER, IDIFEDER/2018/048), Ministry of Science and Innovation (MCIN and NextGenEU PCI2022-135018-2, MICIN and FEDER PID2021-125273NB, RYC2019-028510-I, RYC2020-030254-I, RYC2021-031273-I, RYC2022-038164-I); Sweden: Carl Trygger Foundation (Carl Trygger Foundation CTS 22:2312), Swedish Research Council (Swedish Research Council 2023-04654, VR 2018-00482, VR 2022-03845, VR 2022-04683, VR 2023-03403, VR Grant No. 2021-03651), Knut and Alice Wallenberg Foundation (KAW 2018.0458, KAW 2019.0447, KAW 2022.0358); Switzerland: Swiss National Science Foundation (SNSF—PCEFP2_194658); United Kingdom: Leverhulme Trust (Leverhulme Trust RPG-2020-004), Royal Society (NIF-R1-231091); USA: U.S. Department of Energy (ECA DE-AC02-76SF00515), Neubauer Family Foundation.

DATA AVAILABILITY

No data were created or analyzed in this study.

[1] L. Evans and P. Bryant, LHC machine, J. Instrum. **3**, S08001 (2008).
[2] ATLAS Collaboration, Observation of a new particle in the search for the Standard Model Higgs boson with the ATLAS detector at the LHC, Phys. Lett. B **716**, 1 (2012).
[3] CMS Collaboration, Observation of a new boson at a mass of 125 GeV with the CMS experiment at the LHC, Phys. Lett. B **716**, 30 (2012).
[4] CMS Collaboration, A measurement of the Higgs boson mass in the diphoton decay channel, Phys. Lett. B **805**, 135425 (2020).
[5] ATLAS Collaboration, Combined measurement of the Higgs boson mass from the $H \to \gamma\gamma$ and $H \to ZZ^* \to 4\ell$ decay channels with the ATLAS detector using $\sqrt{s} = 7$, 8, and 13 TeV pp collision data, Phys. Rev. Lett. **131**, 251802 (2023).
[6] CMS Collaboration, Measurement of the Higgs boson mass and width using the four-lepton final state in proton-proton collisions at $\sqrt{s} = 13$ TeV, arXiv:2409.13663.
[7] A. Djouadi, The anatomy of electroweak symmetry breaking tome II: The Higgs bosons in the minimal supersymmetric model, Phys. Rep. **459**, 1 (2008).
[8] G. C. Branco, P. M. Ferreira, L. Lavoura, M. N. Rebelo, M. Sher, and J. P. Silva, Theory and phenomenology of two-Higgs-doublet models, Phys. Rep. **516**, 1 (2012).
[9] G. Senjanovic and R. N. Mohapatra, Exact left-right symmetry and spontaneous violation of parity, Phys. Rev. D **12**, 1502 (1975).
[10] J. E. Cieza Montalvo, N. V. Cortez, J. Sa Borges, and M. D. Tonasse, Searching for doubly charged Higgs bosons at the LHC in a 3-3-1 model, Nucl. Phys. **B756**, 1 (2006).
[11] J. F. Gunion, R. Vega, and J. Wudka, Higgs triplets in the Standard Model, Phys. Rev. D **42**, 1673 (1990).
[12] H. Georgi and M. Machacek, Doubly charged Higgs bosons, Nucl. Phys. **B262**, 463 (1985).
[13] C. Degrande, M. Ubiali, M. Wiesemann, and M. Zaro, Heavy charged Higgs boson production at the LHC, J. High Energy Phys. 10 (2015) 145.
[14] C. Degrande, R. Frederix, V. Hirschi, M. Ubiali, M. Wiesemann, and M. Zaro, Accurate predictions for charged Higgs production: Closing the $m_{H^\pm} \sim m_t$ window, Phys. Lett. B **772**, 87 (2017).
[15] ALEPH, DELPHI, L3, OPAL, and LEP Collaborations, Search for charged Higgs bosons: Combined results using LEP data, Eur. Phys. J. C **73**, 2463 (2013).
[16] ATLAS Collaboration, Search for charged Higgs bosons decaying via $H^\pm \to \tau\nu$ in $t\bar{t}$ events using pp collision data at $\sqrt{s} = 7$ TeV with the ATLAS detector, J. High Energy Phys. 06 (2012) 039.

[17] ATLAS Collaboration, Search for charged Higgs bosons through the violation of lepton universality in $t\bar{t}$ events using pp collision data at $\sqrt{s} = 7$ TeV with the ATLAS experiment, J. High Energy Phys. 03 (2013) 076.
[18] ATLAS Collaboration, Search for charged Higgs bosons decaying via $H^{\pm} \to \tau^{\pm}\nu$ in fully hadronic final states using pp collision data at $\sqrt{s} = 8$ TeV with the ATLAS detector, J. High Energy Phys. 03 (2015) 088.
[19] CMS Collaboration, Search for a light charged Higgs boson in top quark decays in pp collisions at $\sqrt{s} = 7$ TeV, J. High Energy Phys. 07 (2012) 143.
[20] CMS Collaboration, Search for a charged Higgs boson in pp collisions at $\sqrt{s} = 8$ TeV, J. High Energy Phys. 11 (2015) 018.
[21] CMS Collaboration, Search for a charged Higgs boson decaying to charm and bottom quarks in proton–proton collisions at $\sqrt{s} = 8$ TeV, J. High Energy Phys. 11 (2018) 115.
[22] ATLAS Collaboration, Search for a light charged Higgs boson in the decay channel $H^{+} \to c\bar{s}$ in $t\bar{t}$ events using pp collisions at $\sqrt{s} = 7$ TeV with the ATLAS detector, Eur. Phys. J. C **73**, 2465 (2013).
[23] CMS Collaboration, Search for a light charged Higgs boson decaying to $c\bar{s}$ in pp collisions at $\sqrt{s} = 8$ TeV, J. High Energy Phys. 12 (2015) 178.
[24] ATLAS Collaboration, Search for charged Higgs bosons in the $H^{\pm} \to tb$ decay channel in pp collisions at $\sqrt{s} = 8$ TeV using the ATLAS detector, J. High Energy Phys. 03 (2016) 127.
[25] ATLAS Collaboration, Search for a charged Higgs boson produced in the vector-boson fusion mode with decay $H^{\pm} \to W^{\pm}Z$ using pp collisions at $\sqrt{s} = 8$ TeV with the ATLAS experiment, Phys. Rev. Lett. **114**, 231801 (2015).
[26] ATLAS Collaboration, Search for charged Higgs bosons decaying via $H^{\pm} \to \tau^{\pm}\nu_{\tau}$ in the τ^{+} jets and τ^{+}lepton final states with 36 fb^{-1} of pp collision data recorded at $\sqrt{s} =$ 13 TeV with the ATLAS experiment, J. High Energy Phys. 09 (2018) 139.
[27] CMS Collaboration, Search for charged Higgs bosons in the $H^{\pm} \to \tau^{\pm}\nu_{\tau}$ decay channel in proton–proton collisions at $\sqrt{s} = 13$ TeV, J. High Energy Phys. 07 (2019) 142.
[28] ATLAS Collaboration, Search for charged Higgs bosons decaying into a top quark and a bottom quark at $\sqrt{s} =$ 13 TeV with the ATLAS detector, J. High Energy Phys. 06 (2021) 145.
[29] CMS Collaboration, Search for charged Higgs bosons decaying into a top and a bottom quark in the all-jet final state of pp collisions at $\sqrt{s} = 13$ TeV, J. High Energy Phys. 07 (2020) 126.
[30] ATLAS Collaboration, Search for resonant WZ production in the fully leptonic final state in proton–proton collisions at $\sqrt{s} = 13$ TeV with the ATLAS detector, Phys. Lett. B **787**, 68 (2018).
[31] CMS Collaboration, Search for charged Higgs bosons produced in vector boson fusion processes and decaying into vector boson pairs in proton–proton collisions at $\sqrt{s} = 13$ TeV, Eur. Phys. J. C **81**, 723 (2021).
[32] CMS Collaboration, Search for a charged Higgs boson decaying into a heavy neutral Higgs boson and a W boson in proton-proton collisions at $\sqrt{s} = 13$ TeV, J. High Energy Phys. 09 (2023) 032.
[33] ATLAS Collaboration, Search for a heavy charged Higgs boson decaying into a W boson and a Higgs boson in final states with leptons and b-jets in $\sqrt{s} = 13$ TeV pp collisions with the ATLAS detector, arXiv:2411.03969.
[34] ATLAS Collaboration, Search for a light charged Higgs boson in $t \to H^{\pm}b$ decays, with $H^{\pm} \to cb$, in the lepton + jets final state in proton–proton collisions at $\sqrt{s} = 13$ TeV with the ATLAS detector, J. High Energy Phys. 09 (2023) 004.
[35] CMS Collaboration, Search for a light charged Higgs boson in the $H^{\pm} \to cs$ channel in proton–proton collisions at $\sqrt{s} = 13$ TeV, Phys. Rev. D **102**, 072001 (2020).
[36] ATLAS Collaboration, Search for a light charged Higgs boson in $t \to H^{\pm}b$ decays, with $H^{\pm} \to cs$, in pp collisions at $\sqrt{s} = 13$ TeV with the ATLAS detector, Eur. Phys. J. C **85**, 153 (2025).
[37] ATLAS Collaboration, Search for heavy Higgs bosons decaying into two tau leptons with the ATLAS detector using pp collisions at $\sqrt{s} = 13$ TeV, Phys. Rev. Lett. **125**, 051801 (2020).
[38] CMS Collaboration, Searches for additional Higgs bosons and for vector leptoquarks in $\tau\tau$ final states in proton–proton collisions at $\sqrt{s} = 13$ TeV, J. High Energy Phys. 07 (2023) 073.
[39] A. Djouadi, L. Maiani, G. Moreau, A. Polosa, J. Quevillon, and V. Riquer, The post-Higgs MSSM scenario: Habemus MSSM?, Eur. Phys. J. C **73**, 2650 (2013).
[40] A. Djouadi, L. Maiani, A. Polosa, J. Quevillon, and V. Riquer, Fully covering the MSSM Higgs sector at the LHC, J. High Energy Phys. 06 (2015) 168.
[41] Heavy Flavor Averaging Group, HFLAV semileptonic HF results: $R(D)$ and $R(D^{*})$ ratios, https://hflav-eos.web.cern.ch/hflav-eos/semi/moriond24/html/RDsDsstar/RDRDs.html (2024).
[42] J. Hernandez-Sanchez, S. Moretti, R. Noriega-Papaqui, and A. Rosado, Off-diagonal terms in Yukawa textures of the type-III 2-Higgs doublet model and light charged Higgs boson phenomenology, J. High Energy Phys. 07 (2013) 044.
[43] S. Iguro and K. Tobe, $R(D^{(*)})$ in a general two Higgs doublet model, Nucl. Phys. **B925**, 560 (2017).
[44] W. Altmannshofer, P. S. Bhupal Dev, and A. Soni, $R_{D^{(*)}}$ anomaly: A possible hint for natural supersymmetry with R-parity violation, Phys. Rev. D **96**, 095010 (2017).
[45] E. Bagnaschi *et al.*, MSSM Higgs boson searches at the LHC: Benchmark scenarios for Run 2 and beyond, Eur. Phys. J. C **79**, 617 (2019).
[46] Y. Freund and R. E. Schapire, A decision-theoretic generalization of on-line learning and an application to boosting, J. Comput. Syst. Sci. **55**, 119 (1997).
[47] P. Baldi, K. Cranmer, T. Faucett, P. Sadowski, and D. Whiteson, Parameterized neural networks for high-energy physics, Eur. Phys. J. C **76**, 235 (2016).
[48] ATLAS Collaboration, The ATLAS experiment at the CERN Large Hadron Collider, J. Instrum. **3**, S08003 (2008).
[49] G. Avoni *et al.*, The new LUCID-2 detector for luminosity measurement and monitoring in ATLAS, J. Instrum. **13**, P07017 (2018).

[50] ATLAS Collaboration, Performance of the ATLAS trigger system in 2015, Eur. Phys. J. C **77**, 317 (2017).

[51] ATLAS Collaboration, Software and computing for Run 3 of the ATLAS experiment at the LHC, arXiv:2404.06335.

[52] ATLAS Collaboration, Luminosity determination in pp collisions at $\sqrt{s} = 13$ TeV using the ATLAS detector at the LHC, Eur. Phys. J. C **83**, 982 (2023).

[53] S. Agostinelli *et al.*, Geant4—A simulation toolkit, Nucl. Instrum. Methods Phys. Res., Sect. A **506**, 250 (2003).

[54] ATLAS Collaboration, The ATLAS simulation infrastructure, Eur. Phys. J. C **70**, 823 (2010).

[55] T. Sjöstrand, S. Mrenna, and P. Z. Skands, A brief introduction to Pythia 8.1, Comput. Phys. Commun. **178**, 852 (2008).

[56] ATLAS Collaboration, The Pythia 8 A3 tune description of ATLAS minimum bias and inelastic measurements incorporating the Donnachie–Landshoff diffractive model, Technical Report No. ATL-PHYS-PUB-2016-017, CERN, 2016, https://cds.cern.ch/record/2206965.

[57] R. D. Ball *et al.* (NNPDF Collaboration), Parton distributions with LHC data, Nucl. Phys. **B867**, 244 (2013).

[58] S. Alioli, P. Nason, C. Oleari, and E. Re, A general framework for implementing NLO calculations in shower Monte Carlo programs: The POWHEG BOX, J. High Energy Phys. 06 (2010) 043.

[59] T. Sjöstrand, S. Ask, J. R. Christiansen, R. Corke, N. Desai, P. Ilten, S. Mrenna, S. Prestel, C. O. Rasmussen, and P. Z. Skands, An introduction to Pythia 8.2, Comput. Phys. Commun. **191**, 159 (2015).

[60] R. D. Ball *et al.* (NNPDF Collaboration), Parton distributions for the LHC run II, J. High Energy Phys. 04 (2015) 040.

[61] E. Bothmann *et al.*, Event generation with Sherpa 2.2, SciPost Phys. **7**, 034 (2019).

[62] H.-L. Lai, M. Guzzi, J. Huston, Z. Li, P. M. Nadolsky, J. Pumplin, and C.-P. Yuan, New parton distributions for collider physics, Phys. Rev. D **82**, 074024 (2010).

[63] J. Alwall, R. Frederix, S. Frixione, V. Hirschi, F. Maltoni, O. Mattelaer, H.-S. Shao, T. Stelzer, P. Torrielli, and M. Zaro, The automated computation of tree-level and next-to-leading order differential cross sections, and their matching to parton shower simulations, J. High Energy Phys. 07 (2014) 079.

[64] ATLAS Collaboration, ATLAS Pythia 8 tunes to 7 TeV data, Report No. ATL-PHYS-PUB-2014-021, 2014, https://cds.cern.ch/record/1966419.

[65] ATLAS Collaboration, Vertex reconstruction performance of the ATLAS detector at $\sqrt{s} = 13$ TeV, Report No. ATL-PHYS-PUB-2015-026, 2015, https://cds.cern.ch/record/2037717.

[66] ATLAS Collaboration, ATLAS data quality operations and performance for 2015–2018 data-taking, J. Instrum. **15**, P04003 (2020).

[67] ATLAS Collaboration, Reconstruction, energy calibration, and identification of hadronically decaying tau leptons in the ATLAS experiment for Run-2 of the LHC, Report No. ATL-PHYS-PUB-2015-045, 2015, https://cds.cern.ch/record/2064383.

[68] ATLAS Collaboration, Identification of hadronic tau lepton decays using neural networks in the ATLAS experiment, Report No. ATL-PHYS-PUB-2019-033, 2019, https://cds.cern.ch/record/2688062.

[69] ATLAS Collaboration, Measurement of the tau lepton reconstruction and identification performance in the ATLAS experiment using pp collisions at $\sqrt{s} = 13$ TeV, Report No. ATLAS-CONF-2017-029, 2017, https://cds.cern.ch/record/2261772.

[70] ATLAS Collaboration, Electron and photon efficiencies in LHC Run 2 with the ATLAS experiment, J. High Energy Phys. 05 (2024) 162.

[71] ATLAS Collaboration, Muon reconstruction and identification efficiency in ATLAS using the full Run $2pp$ collision data set at $\sqrt{s} = 13$ TeV, Eur. Phys. J. C **81**, 578 (2021).

[72] ATLAS Collaboration, Jet reconstruction and performance using particle flow with the ATLAS Detector, Eur. Phys. J. C **77**, 466 (2017).

[73] M. Cacciari, G. P. Salam, and G. Soyez, The anti-k_t jet clustering algorithm, J. High Energy Phys. 04 (2008) 063.

[74] M. Cacciari, G. P. Salam, and G. Soyez, FastJet user manual, Eur. Phys. J. C **72**, 1896 (2012).

[75] ATLAS Collaboration, ATLAS flavour-tagging algorithms for the LHC Run $2pp$ collision dataset, Eur. Phys. J. C **83**, 681 (2023).

[76] ATLAS Collaboration, The performance of missing transverse momentum reconstruction and its significance with the ATLAS detector using 140 fb^{-1} of $\sqrt{s} = 13$ TeV pp collisions, arXiv:2402.05858.

[77] ATLAS Collaboration, Performance of the missing transverse momentum triggers for the ATLAS detector during Run-2 data taking, J. High Energy Phys. 08 (2020) 080.

[78] ATLAS Collaboration, Search for charged Higgs bosons produced in association with a top quark and decaying via $H^{\pm} \to \tau\nu$ using pp collision data recorded at $\sqrt{s} = 13$ TeV by the ATLAS detector, Phys. Lett. B **759**, 555 (2016).

[79] ATLAS Collaboration, Performance of electron and photon triggers in ATLAS during LHC Run 2, Eur. Phys. J. C **80**, 47 (2020).

[80] ATLAS Collaboration, Performance of the ATLAS muon triggers in Run 2, J. Instrum. **15**, P09015 (2020).

[81] ATLAS Collaboration, The ATLAS inner detector trigger performance in pp collisions at 13 TeV during LHC Run 2, Eur. Phys. J. C **82**, 206 (2022).

[82] ATLAS Collaboration, The performance of the jet trigger for the ATLAS detector during 2011 data taking, Eur. Phys. J. C **76**, 526 (2016).

[83] F. Chollet *et al.*, Keras, https://keras.io (2015).

[84] Martín Abadi *et al.*, TensorFlow: Large-scale machine learning on heterogeneous systems, Software available from https://www.tensorflow.org (2015).

[85] M. Stone, Cross-validatory choice and assessment of statistical predictions, J. R. Stat. Soc. Ser. B **36**, 111 (1974).

[86] ATLAS Collaboration, Measurement of τ polarization in $W \to \tau\nu$ decays with the ATLAS detector in pp collisions at $\sqrt{s} = 7$ TeV, Eur. Phys. J. C **72**, 2062 (2012).

[87] J. Bellm *et al.*, Herwig7.0/Herwig++ 3.0 release note, Eur. Phys. J. C **76**, 196 (2016).

[88] ATLAS Collaboration, Luminosity determination in pp collisions at $\sqrt{s} = 13$ TeV using the ATLAS detector at the LHC, Eur. Phys. J. C **83**, 982 (2023).

[89] G. Cowan, K. Cranmer, E. Gross, and O. Vitells, Asymptotic formulae for likelihood-based tests of new physics, Eur. Phys. J. C **71**, 1554 (2011); **73**, 2501(E) (2013).
[90] A. L. Read, Presentation of search results: The CL_S technique, J. Phys. G **28**, 2693 (2002).
[91] J. R. Andersen *et al.*, Handbook of LHC Higgs cross sections: 3. Higgs properties, arXiv:1307.1347.
[92] ATLAS Collaboration, ATLAS computing acknowledgements, Report No. ATL-SOFT-PUB-2025-001, 2025, https://cds.cern.ch/record/2922210.

G. Aad,[104] E. Aakvaag,[17] B. Abbott,[123] S. Abdelhameed,[119a] K. Abeling,[56] N. J. Abicht,[50] S. H. Abidi,[30] M. Aboelela,[46] A. Aboulhorma,[36e] H. Abramowicz,[155] Y. Abulaiti,[120] B. S. Acharya,[70a,70b,b] A. Ackermann,[64a] C. Adam Bourdarios,[4] L. Adamczyk,[87a] S. V. Addepalli,[147] M. J. Addison,[103] J. Adelman,[118] A. Adiguzel,[22c] T. Adye,[137] A. A. Affolder,[139] Y. Afik,[41] M. N. Agaras,[13] A. Aggarwal,[102] C. Agheorghiesei,[28c] F. Ahmadov,[40,c] S. Ahuja,[97] X. Ai,[63e] G. Aielli,[77a,77b] A. Aikot,[167] M. Ait Tamlihat,[36e] B. Aitbenchikh,[36a] M. Akbiyik,[102] T. P. A. Åkesson,[100] A. V. Akimov,[149] D. Akiyama,[172] N. N. Akolkar,[25] S. Aktas,[22a] G. L. Alberghi,[24b] J. Albert,[169] P. Albicocco,[54] G. L. Albouy,[61] S. Alderweireldt,[53] Z. L. Alegria,[124] M. Aleksa,[37] I. N. Aleksandrov,[40] C. Alexa,[28b] T. Alexopoulos,[10] F. Alfonsi,[24b] M. Algren,[57] M. Alhroob,[171] B. Ali,[135] H. M. J. Ali,[93,d] S. Ali,[32] S. W. Alibocus,[94] M. Aliev,[34c] G. Alimonti,[72a] W. Alkakhi,[56] C. Allaire,[67] B. M. M. Allbrooke,[150] J. S. Allen,[103] J. F. Allen,[53] C. A. Allendes Flores,[140f] P. P. Allport,[21] A. Aloisio,[73a,73b] F. Alonso,[92] C. Alpigiani,[142] Z. M. K. Alsolami,[93] A. Alvarez Fernandez,[102] M. Alves Cardoso,[57] M. G. Alviggi,[73a,73b] M. Aly,[103] Y. Amaral Coutinho,[84b] A. Ambler,[106] C. Amelung,[37] M. Amerl,[103] C. G. Ames,[111] D. Amidei,[108] B. Amini,[55] K. Amirie,[158] A. Amirkhanov,[39] S. P. Amor Dos Santos,[133a] K. R. Amos,[167] D. Amperiadou,[156] S. An,[85] V. Ananiev,[128] C. Anastopoulos,[143] T. Andeen,[11] J. K. Anders,[94] A. C. Anderson,[60] A. Andreazza,[72a,72b] S. Angelidakis,[9] A. Angerami,[43] A. V. Anisenkov,[39] A. Annovi,[75a] C. Antel,[57] E. Antipov,[149] M. Antonelli,[54] F. Anulli,[76a] M. Aoki,[85] T. Aoki,[157] M. A. Aparo,[150] L. Aperio Bella,[49] C. Appelt,[155] A. Apyan,[27] S. J. Arbiol Val,[88] C. Arcangeletti,[54] A. T. H. Arce,[52] J-F. Arguin,[110] S. Argyropoulos,[156] J.-H. Arling,[49] O. Arnaez,[4] H. Arnold,[149] G. Artoni,[76a,76b] H. Asada,[113] K. Asai,[121] S. Asai,[157] N. A. Asbah,[37] R. A. Ashby Pickering,[171] A. M. Aslam,[97] K. Assamagan,[30] R. Astalos,[29a] K. S. V. Astrand,[100] S. Atashi,[162] R. J. Atkin,[34a] H. Atmani,[36f] P. A. Atmasiddha,[131] K. Augsten,[135] A. D. Auriol,[42] V. A. Austrup,[103] G. Avolio,[37] K. Axiotis,[57] G. Azuelos,[110,e] D. Babal,[29b] H. Bachacou,[138] K. Bachas,[156,f] A. Bachiu,[35] E. Bachmann,[51] A. Badea,[41] T. M. Baer,[108] P. Bagnaia,[76a,76b] M. Bahmani,[19] D. Bahner,[55] H. Bahrasemani,[146] K. Bai,[126] J. T. Baines,[137] L. Baines,[96] O. K. Baker,[176] E. Bakos,[16] D. Bakshi Gupta,[8] L. E. Balabram Filho,[84b] V. Balakrishnan,[123] R. Balasubramanian,[4] E. M. Baldin,[39] P. Balek,[87a] E. Ballabene,[24b,24a] F. Balli,[138] L. M. Baltes,[64a] W. K. Balunas,[33] J. Balz,[102] I. Bamwidhi,[119b] E. Banas,[88] M. Bandieramonte,[132] A. Bandyopadhyay,[25] S. Bansal,[25] L. Barak,[155] M. Barakat,[49] E. L. Barberio,[107] D. Barberis,[58b,58a] M. Barbero,[104] M. Z. Barel,[117] T. Barillari,[112] M-S. Barisits,[37] T. Barklow,[147] P. Baron,[125] D. A. Baron Moreno,[103] A. Baroncelli,[63a] A. J. Barr,[129] J. D. Barr,[98] F. Barreiro,[101] J. Barreiro Guimarães da Costa,[14] M. G. Barros Teixeira,[133a] S. Barsov,[39] F. Bartels,[64a] R. Bartoldus,[147] A. E. Barton,[93] P. Bartos,[29a] A. Basan,[102] M. Baselga,[50] S. Bashiri,[88] A. Bassalat,[67,g] M. J. Basso,[159a] S. Bataju,[46] R. Bate,[168] R. L. Bates,[60] S. Batlamous,[101] M. Battaglia,[139] D. Battulga,[19] M. Bauce,[76a,76b] M. Bauer,[80] P. Bauer,[25] L. T. Bazzano Hurrell,[31] J. B. Beacham,[112] T. Beau,[130] J. Y. Beaucamp,[92] P. H. Beauchemin,[161] P. Bechtle,[25] H. P. Beck,[20,h] K. Becker,[171] A. J. Beddall,[83] V. A. Bednyakov,[40] C. P. Bee,[149] L. J. Beemster,[16] M. Begalli,[84d] M. Begel,[30] J. K. Behr,[49] J. F. Beirer,[37] F. Beisiegel,[25] M. Belfkir,[119b] G. Bella,[155] L. Bellagamba,[24b] A. Bellerive,[35] P. Bellos,[21] K. Beloborodov,[39] D. Benchekroun,[36a] F. Bendebba,[36a] Y. Benhammou,[155] K. C. Benkendorfer,[62] L. Beresford,[49] M. Beretta,[54] E. Bergeaas Kuutmann,[165] N. Berger,[4] B. Bergmann,[135] J. Beringer,[18a] G. Bernardi,[5] C. Bernius,[147] F. U. Bernlochner,[25] F. Bernon,[37] A. Berrocal Guardia,[13] T. Berry,[97] P. Berta,[136] A. Berthold,[51] S. Bethke,[112] A. Betti,[76a,76b] A. J. Bevan,[96] N. K. Bhalla,[55] S. Bharthuar,[112] S. Bhatta,[149] D. S. Bhattacharya,[170] P. Bhattarai,[147] Z. M. Bhatti,[120] K. D. Bhide,[55] V. S. Bhopatkar,[124] R. M. Bianchi,[132] G. Bianco,[24b,24a] O. Biebel,[111] M. Biglietti,[78a] C. S. Billingsley,[46] Y. Bimgdi,[36f] M. Bindi,[56] A. Bingham,[175] A. Bingul,[22b] C. Bini,[76a,76b] G. A. Bird,[33] M. Birman,[173] M. Biros,[136] S. Biryukov,[150] T. Bisanz,[50] E. Bisceglie,[45b,45a]

J. P. Biswal,[137] D. Biswas,[145] I. Bloch,[49] A. Blue,[60] U. Blumenschein,[96] J. Blumenthal,[102] V. S. Bobrovnikov,[39] M. Boehler,[55] B. Boehm,[170] D. Bogavac,[37] A. G. Bogdanchikov,[39] L. S. Boggia,[130] V. Boisvert,[97] P. Bokan,[37] T. Bold,[87a] M. Bomben,[5] M. Bona,[96] M. Boonekamp,[138] A. G. Borbély,[60] I. S. Bordulev,[39] G. Borissov,[93] D. Bortoletto,[129] D. Boscherini,[24b] M. Bosman,[13] K. Bouaouda,[36a] N. Bouchhar,[167] L. Boudet,[4] J. Boudreau,[132] E. V. Bouhova-Thacker,[93] D. Boumediene,[42] R. Bouquet,[58b,58a] A. Boveia,[122] J. Boyd,[37] D. Boye,[30] I. R. Boyko,[40] L. Bozianu,[57] J. Bracinik,[21] N. Brahimi,[4] G. Brandt,[175] O. Brandt,[33] B. Brau,[105] J. E. Brau,[126] R. Brener,[173] L. Brenner,[117] R. Brenner,[165] S. Bressler,[173] G. Brianti,[79a,79b] D. Britton,[60] D. Britzger,[112] I. Brock,[25] R. Brock,[109] G. Brooijmans,[43] A. J. Brooks,[69] E. M. Brooks,[159b] E. Brost,[30] L. M. Brown,[169] L. E. Bruce,[62] T. L. Bruckler,[129] P. A. Bruckman de Renstrom,[88] B. Brüers,[49] A. Bruni,[24b] G. Bruni,[24b] D. Brunner,[48a,48b] M. Bruschi,[24b] N. Bruscino,[76a,76b] T. Buanes,[17] Q. Buat,[142] D. Buchin,[112] A. G. Buckley,[60] O. Bulekov,[39] B. A. Bullard,[147] S. Burdin,[94] C. D. Burgard,[50] A. M. Burger,[37] B. Burghgrave,[8] O. Burlayenko,[55] J. Burleson,[166] J. T. P. Burr,[33] J. C. Burzynski,[146] E. L. Busch,[43] V. Büscher,[102] P. J. Bussey,[60] J. M. Butler,[26] C. M. Buttar,[60] J. M. Butterworth,[98] W. Buttinger,[137] C. J. Buxo Vazquez,[109] A. R. Buzykaev,[39] S. Cabrera Urbán,[167] L. Cadamuro,[67] D. Caforio,[59] H. Cai,[132] Y. Cai,[24b,114c,24a] Y. Cai,[114a] V. M. M. Cairo,[37] O. Cakir,[3a] N. Calace,[37] P. Calafiura,[18a] G. Calderini,[130] P. Calfayan,[35] G. Callea,[60] L. P. Caloba,[84b] D. Calvet,[42] S. Calvet,[42] R. Camacho Toro,[130] S. Camarda,[37] D. Camarero Munoz,[27] P. Camarri,[77a,77b] M. T. Camerlingo,[73a,73b] D. Cameron,[37] C. Camincher,[169] M. Campanelli,[98] A. Camplani,[44] V. Canale,[73a,73b] A. C. Canbay,[3a] E. Canonero,[97] J. Cantero,[167] Y. Cao,[166] F. Capocasa,[27] M. Capua,[45b,45a] A. Carbone,[72a,72b] R. Cardarelli,[77a] J. C. J. Cardenas,[8] M. P. Cardiff,[27] G. Carducci,[45b,45a] T. Carli,[37] G. Carlino,[73a] J. I. Carlotto,[13] B. T. Carlson,[132,i] E. M. Carlson,[169] J. Carmignani,[94] L. Carminati,[72a,72b] A. Carnelli,[138] M. Carnesale,[37] S. Caron,[116] E. Carquin,[140f] I. B. Carr,[107] S. Carrá,[72a] G. Carratta,[24b,24a] A. M. Carroll,[126] M. P. Casado,[13,j] M. Caspar,[49] F. L. Castillo,[4] L. Castillo Garcia,[13] V. Castillo Gimenez,[167] N. F. Castro,[133a,133e] A. Catinaccio,[37] J. R. Catmore,[128] T. Cavaliere,[4] V. Cavaliere,[30] L. J. Caviedes Betancourt,[23b] Y. C. Cekmecelioglu,[49] E. Celebi,[83] S. Cella,[37] V. Cepaitis,[57] K. Cerny,[125] A. S. Cerqueira,[84a] A. Cerri,[75a,75b] L. Cerrito,[77a,77b] F. Cerutti,[18a] B. Cervato,[145] A. Cervelli,[24b] G. Cesarini,[54] S. A. Cetin,[83] P. M. Chabrillat,[130] J. Chan,[18a] W. Y. Chan,[157] J. D. Chapman,[33] E. Chapon,[138] B. Chargeishvili,[153b] D. G. Charlton,[21] C. Chauhan,[136] Y. Che,[114a] S. Chekanov,[6] S. V. Chekulaev,[159a] G. A. Chelkov,[40,k] B. Chen,[155] B. Chen,[169] H. Chen,[114a] H. Chen,[30] J. Chen,[63c] J. Chen,[146] M. Chen,[129] S. Chen,[89] S. J. Chen,[114a] X. Chen,[63c] X. Chen,[15,l] Y. Chen,[63a] C. L. Cheng,[174] H. C. Cheng,[65a] S. Cheong,[147] A. Cheplakov,[40] E. Cheremushkina,[49] E. Cherepanova,[117] R. Cherkaoui El Moursli,[36e] E. Cheu,[7] K. Cheung,[66] L. Chevalier,[138] V. Chiarella,[54] G. Chiarelli,[75a] N. Chiedde,[104] G. Chiodini,[71a] A. S. Chisholm,[21] A. Chitan,[28b] M. Chitishvili,[167] M. V. Chizhov,[40,m] K. Choi,[11] Y. Chou,[142] E. Y. S. Chow,[116] K. L. Chu,[173] M. C. Chu,[65a] X. Chu,[14,114c] Z. Chubinidze,[54] J. Chudoba,[134] J. J. Chwastowski,[88] D. Cieri,[112] K. M. Ciesla,[87a] V. Cindro,[95] A. Ciocio,[18a] F. Cirotto,[73a,73b] Z. H. Citron,[173] M. Citterio,[72a] D. A. Ciubotaru,[28b] A. Clark,[57] P. J. Clark,[53] N. Clarke Hall,[98] C. Clarry,[158] S. E. Clawson,[49] C. Clement,[48a,48b] Y. Coadou,[104] M. Cobal,[70a,70c] A. Coccaro,[58b] R. F. Coelho Barrue,[133a] R. Coelho Lopes De Sa,[105] S. Coelli,[72a] L. S. Colangeli,[158] B. Cole,[43] J. Collot,[61] P. Conde Muiño,[133a,133g] M. P. Connell,[34c] S. H. Connell,[34c] E. I. Conroy,[129] F. Conventi,[73a,n] H. G. Cooke,[21] A. M. Cooper-Sarkar,[129] F. A. Corchia,[24b,24a] A. Cordeiro Oudot Choi,[130] L. D. Corpe,[42] M. Corradi,[76a,76b] F. Corriveau,[106,o] A. Cortes-Gonzalez,[19] M. J. Costa,[167] F. Costanza,[4] D. Costanzo,[143] B. M. Cote,[122] J. Couthures,[4] G. Cowan,[97] K. Cranmer,[174] L. Cremer,[50] D. Cremonini,[24b,24a] S. Crépé-Renaudin,[61] F. Crescioli,[130] M. Cristinziani,[145] M. Cristoforetti,[79a,79b] V. Croft,[117] J. E. Crosby,[124] G. Crosetti,[45b,45a] A. Cueto,[101] H. Cui,[98] Z. Cui,[7] W. R. Cunningham,[60] F. Curcio,[167] J. R. Curran,[53] P. Czodrowski,[37] M. J. Da Cunha Sargedas De Sousa,[58b,58a] J. V. Da Fonseca Pinto,[84b] C. Da Via,[103] W. Dabrowski,[87a] T. Dado,[37] S. Dahbi,[152] T. Dai,[108] D. Dal Santo,[20] C. Dallapiccola,[105] M. Dam,[44] G. D'amen,[30] V. D'Amico,[111] J. Damp,[102] J. R. Dandoy,[35] D. Dannheim,[37] M. Danninger,[146] V. Dao,[149] G. Darbo,[58b] S. J. Das,[30] F. Dattola,[49] S. D'Auria,[72a,72b] A. D'Avanzo,[73a,73b] T. Davidek,[136] I. Dawson,[96] H. A. Day-hall,[135] K. De,[8] C. De Almeida Rossi,[158] R. De Asmundis,[73a] N. De Biase,[49] S. De Castro,[24b,24a] N. De Groot,[116] P. de Jong,[117] H. De la Torre,[118] A. De Maria,[114a] A. De Salvo,[76a] U. De Sanctis,[77a,77b] F. De Santis,[71a,71b] A. De Santo,[150] J. B. De Vivie De Regie,[61] J. Debevc,[95] D. V. Dedovich,[40] J. Degens,[94] A. M. Deiana,[46] J. Del Peso,[101] L. Delagrange,[130] F. Deliot,[138] C. M. Delitzsch,[50]

M. Della Pietra,[73a,73b] D. Della Volpe,[57] A. Dell'Acqua,[37] L. Dell'Asta,[72a,72b] M. Delmastro,[4] C. C. Delogu,[102] P. A. Delsart,[61] S. Demers,[176] M. Demichev,[40] S. P. Denisov,[39] H. Denizli,[22a,p] L. D'Eramo,[42] D. Derendarz,[88] F. Derue,[130] P. Dervan,[94] K. Desch,[25] C. Deutsch,[25] F. A. Di Bello,[58b,58a] A. Di Ciaccio,[77a,77b] L. Di Ciaccio,[4] A. Di Domenico,[76a,76b] C. Di Donato,[73a,73b] A. Di Girolamo,[37] G. Di Gregorio,[37] A. Di Luca,[79a,79b] B. Di Micco,[78a,78b] R. Di Nardo,[78a,78b] K. F. Di Petrillo,[41] M. Diamantopoulou,[35] F. A. Dias,[117] T. Dias Do Vale,[146] M. A. Diaz,[140a,140b] A. R. Didenko,[40] M. Didenko,[167] E. B. Diehl,[108] S. Díez Cornell,[49] C. Diez Pardos,[145] C. Dimitriadi,[148] A. Dimitrievska,[21] A. Dimri,[149] J. Dingfelder,[25] T. Dingley,[129] I-M. Dinu,[28b] S. J. Dittmeier,[64b] F. Dittus,[37] M. Divisek,[136] B. Dixit,[94] F. Djama,[104] T. Djobava,[153b] C. Doglioni,[103,100] A. Dohnalova,[29a] Z. Dolezal,[136] K. Domijan,[87a] K. M. Dona,[41] M. Donadelli,[84d] B. Dong,[109] J. Donini,[42] A. D'Onofrio,[73a,73b] M. D'Onofrio,[94] J. Dopke,[137] A. Doria,[73a] N. Dos Santos Fernandes,[133a] P. Dougan,[103] M. T. Dova,[92] A. T. Doyle,[60] M. A. Draguet,[129] M. P. Drescher,[56] E. Dreyer,[173] I. Drivas-koulouris,[10] M. Drnevich,[120] M. Drozdova,[57] D. Du,[63a] T. A. du Pree,[117] F. Dubinin,[39] M. Dubovsky,[29a] E. Duchovni,[173] G. Duckeck,[111] O. A. Ducu,[28b] D. Duda,[53] A. Dudarev,[37] E. R. Duden,[27] M. D'uffizi,[103] L. Duflot,[67] M. Dührssen,[37] I. Duminica,[28g] A. E. Dumitriu,[28b] M. Dunford,[64a] S. Dungs,[50] K. Dunne,[48a,48b] A. Duperrin,[104] H. Duran Yildiz,[3a] M. Düren,[59] A. Durglishvili,[153b] D. Duvnjak,[35] B. L. Dwyer,[118] G. I. Dyckes,[18a] M. Dyndal,[87a] B. S. Dziedzic,[37] Z. O. Earnshaw,[150] G. H. Eberwein,[129] B. Eckerova,[29a] S. Eggebrecht,[56] E. Egidio Purcino De Souza,[84e] L. F. Ehrke,[57] G. Eigen,[17] K. Einsweiler,[18a] T. Ekelof,[165] P. A. Ekman,[100] S. El Farkh,[36b] Y. El Ghazali,[63a] H. El Jarrari,[37] A. El Moussaouy,[36a] V. Ellajosyula,[165] M. Ellert,[165] F. Ellinghaus,[175] N. Ellis,[37] J. Elmsheuser,[30] M. Elsawy,[119a] M. Elsing,[37] D. Emeliyanov,[137] Y. Enari,[85] I. Ene,[18a] S. Epari,[13] P. A. Erland,[88] D. Ernani Martins Neto,[88] M. Errenst,[175] M. Escalier,[67] C. Escobar,[167] E. Etzion,[155] G. Evans,[133a,133b] H. Evans,[69] L. S. Evans,[97] A. Ezhilov,[39] S. Ezzarqtouni,[36a] F. Fabbri,[24b,24a] L. Fabbri,[24b,24a] G. Facini,[98] V. Fadeyev,[139] R. M. Fakhrutdinov,[39] D. Fakoudis,[102] S. Falciano,[76a] L. F. Falda Ulhoa Coelho,[133a] F. Fallavollita,[112] G. Falsetti,[45b,45a] J. Faltova,[136] C. Fan,[166] K. Y. Fan,[65b] Y. Fan,[14] Y. Fang,[14,114c] M. Fanti,[72a,72b] M. Faraj,[70a,70b] Z. Farazpay,[99] A. Farbin,[8] A. Farilla,[78a] T. Farooque,[109] J. N. Farr,[176] S. M. Farrington,[137,53] F. Fassi,[36e] D. Fassouliotis,[9] M. Faucci Giannelli,[77a,77b] W. J. Fawcett,[33] L. Fayard,[67] P. Federic,[136] P. Federicova,[134] O. L. Fedin,[39,k] M. Feickert,[174] L. Feligioni,[104] D. E. Fellers,[126] C. Feng,[63b] Z. Feng,[117] M. J. Fenton,[162] L. Ferencz,[49] R. A. M. Ferguson,[93] P. Fernandez Martinez,[68] M. J. V. Fernoux,[104] J. Ferrando,[93] A. Ferrari,[165] P. Ferrari,[117,116] R. Ferrari,[74a] D. Ferrere,[57] C. Ferretti,[108] M. P. Fewell,[1] D. Fiacco,[76a,76b] F. Fiedler,[102] P. Fiedler,[135] S. Filimonov,[39] A. Filipčič,[95] E. K. Filmer,[159a] F. Filthaut,[116] M. C. N. Fiolhais,[133a,133c,q] L. Fiorini,[167] W. C. Fisher,[109] T. Fitschen,[103] P. M. Fitzhugh,[138] I. Fleck,[145] P. Fleischmann,[108] T. Flick,[175] M. Flores,[34d,r] L. R. Flores Castillo,[65a] L. Flores Sanz De Acedo,[37] F. M. Follega,[79a,79b] N. Fomin,[33] J. H. Foo,[158] A. Formica,[138] A. C. Forti,[103] E. Fortin,[37] A. W. Fortman,[18a] L. Fountas,[9,s] D. Fournier,[67] H. Fox,[93] P. Francavilla,[75a,75b] S. Francescato,[62] S. Franchellucci,[57] M. Franchini,[24b,24a] S. Franchino,[64a] D. Francis,[37] L. Franco,[116] V. Franco Lima,[37] L. Franconi,[49] M. Franklin,[62] G. Frattari,[27] Y. Y. Frid,[155] J. Friend,[60] N. Fritzsche,[37] A. Froch,[57] D. Froidevaux,[37] J. A. Frost,[129] Y. Fu,[109] S. Fuenzalida Garrido,[140f] M. Fujimoto,[104] K. Y. Fung,[65a] E. Furtado De Simas Filho,[84e] M. Furukawa,[157] J. Fuster,[167] A. Gaa,[56] A. Gabrielli,[24b,24a] A. Gabrielli,[158] P. Gadow,[37] G. Gagliardi,[58b,58a] L. G. Gagnon,[18a] S. Gaid,[164] S. Galantzan,[155] J. Gallagher,[1] E. J. Gallas,[129] A. L. Gallen,[165] B. J. Gallop,[137] K. K. Gan,[122] S. Ganguly,[157] Y. Gao,[53] A. Garabaglu,[142] F. M. Garay Walls,[140a,140b] B. Garcia,[30] C. García,[167] A. Garcia Alonso,[117] A. G. Garcia Caffaro,[176] J. E. García Navarro,[167] M. Garcia-Sciveres,[18a] G. L. Gardner,[131] R. W. Gardner,[41] N. Garelli,[161] R. B. Garg,[147] J. M. Gargan,[53] C. A. Garner,[158] C. M. Garvey,[34a] V. K. Gassmann,[161] G. Gaudio,[74a] V. Gautam,[13] P. Gauzzi,[76a,76b] J. Gavranovic,[95] I. L. Gavrilenko,[39] A. Gavrilyuk,[39] C. Gay,[168] G. Gaycken,[126] E. N. Gazis,[10] A. Gekow,[122] C. Gemme,[58b] M. H. Genest,[61] A. D. Gentry,[115] S. George,[97] W. F. George,[21] T. Geralis,[47] A. A. Gerwin,[123] P. Gessinger-Befurt,[37] M. E. Geyik,[175] M. Ghani,[171] K. Ghorbanian,[96] A. Ghosal,[145] A. Ghosh,[162] A. Ghosh,[7] B. Giacobbe,[24b] S. Giagu,[76a,76b] T. Giani,[117] A. Giannini,[63a] S. M. Gibson,[97] M. Gignac,[139] D. T. Gil,[87b] A. K. Gilbert,[87a] B. J. Gilbert,[43] D. Gillberg,[35] G. Gilles,[117] L. Ginabat,[130] D. M. Gingrich,[2,e] M. P. Giordani,[70a,70c] P. F. Giraud,[138] G. Giugliarelli,[70a,70c] D. Giugni,[72a] F. Giuli,[77a,77b] I. Gkialas,[9,s] L. K. Gladilin,[39] C. Glasman,[101] G. Glemža,[49] M. Glisic,[126] I. Gnesi,[45b] Y. Go,[30] M. Goblirsch-Kolb,[37] B. Gocke,[50] D. Godin,[110] B. Gokturk,[22a] S. Goldfarb,[107] T. Golling,[57]

M. G. D. Gololo,[34c] D. Golubkov,[39] J. P. Gombas,[109] A. Gomes,[133a,133b] G. Gomes Da Silva,[145] A. J. Gomez Delegido,[167] R. Gonçalo,[133a] L. Gonella,[21] A. Gongadze,[153c] F. Gonnella,[21] J. L. Gonski,[147] R. Y. González Andana,[53] S. González de la Hoz,[167] R. Gonzalez Lopez,[94] C. Gonzalez Renteria,[18a] M. V. Gonzalez Rodrigues,[49] R. Gonzalez Suarez,[165] S. Gonzalez-Sevilla,[57] L. Goossens,[37] B. Gorini,[37] E. Gorini,[71a,71b] A. Gorišek,[95] T. C. Gosart,[131] A. T. Goshaw,[52] M. I. Gostkin,[40] S. Goswami,[124] C. A. Gottardo,[37] S. A. Gotz,[111] M. Gouighri,[36b] A. G. Goussiou,[142] N. Govender,[34c] R. P. Grabarczyk,[129] I. Grabowska-Bold,[87a] K. Graham,[35] E. Gramstad,[128] S. Grancagnolo,[71a,71b] C. M. Grant,[1,138] P. M. Gravila,[28f] F. G. Gravili,[71a,71b] H. M. Gray,[18a] M. Greco,[112] M. J. Green,[1] C. Grefe,[25] A. S. Grefsrud,[17] I. M. Gregor,[49] K. T. Greif,[162] P. Grenier,[147] S. G. Grewe,[112] A. A. Grillo,[139] K. Grimm,[32] S. Grinstein,[13,t] J.-F. Grivaz,[67] E. Gross,[173] J. Grosse-Knetter,[56] L. Guan,[108] J. G. R. Guerrero Rojas,[167] G. Guerrieri,[37] R. Gugel,[102] J. A. M. Guhit,[108] A. Guida,[19] E. Guilloton,[171] S. Guindon,[37] F. Guo,[14,114c] J. Guo,[63c] L. Guo,[49] L. Guo,[114b,u] Y. Guo,[108] A. Gupta,[50] R. Gupta,[132] S. Gurbuz,[25] S. S. Gurdasani,[49] G. Gustavino,[76a,76b] P. Gutierrez,[123] L. F. Gutierrez Zagazeta,[131] M. Gutsche,[51] C. Gutschow,[98] C. Gwenlan,[129] C. B. Gwilliam,[94] E. S. Haaland,[128] A. Haas,[120] M. Habedank,[60] C. Haber,[18a] H. K. Hadavand,[8] A. Hadef,[51] A. I. Hagan,[93] J. J. Hahn,[145] E. H. Haines,[98] M. Haleem,[170] J. Haley,[124] G. D. Hallewell,[104] L. Halser,[20] K. Hamano,[169] M. Hamer,[25] E. J. Hampshire,[97] J. Han,[63b] L. Han,[114a] L. Han,[63a] S. Han,[18a] K. Hanagaki,[85] M. Hance,[139] D. A. Hangal,[43] H. Hanif,[146] M. D. Hank,[131] J. B. Hansen,[44] P. H. Hansen,[44] D. Harada,[57] T. Harenberg,[175] S. Harkusha,[177] M. L. Harris,[105] Y. T. Harris,[25] J. Harrison,[13] N. M. Harrison,[122] P. F. Harrison,[171] N. M. Hartman,[112] N. M. Hartmann,[111] R. Z. Hasan,[97,137] Y. Hasegawa,[144] F. Haslbeck,[129] S. Hassan,[17] R. Hauser,[109] C. M. Hawkes,[21] R. J. Hawkings,[37] Y. Hayashi,[157] D. Hayden,[109] C. Hayes,[108] R. L. Hayes,[117] C. P. Hays,[129] J. M. Hays,[96] H. S. Hayward,[94] F. He,[63a] M. He,[14,114c] Y. He,[49] Y. He,[98] N. B. Heatley,[96] V. Hedberg,[100] A. L. Heggelund,[128] C. Heidegger,[55] K. K. Heidegger,[55] J. Heilman,[35] S. Heim,[49] T. Heim,[18a] J. G. Heinlein,[131] J. J. Heinrich,[126] L. Heinrich,[112,v] J. Hejbal,[134] A. Held,[174] S. Hellesund,[17] C. M. Helling,[168] S. Hellman,[48a,48b] R. C. W. Henderson,[93] L. Henkelmann,[33] A. M. Henriques Correia,[37] H. Herde,[100] Y. Hernández Jiménez,[149] L. M. Herrmann,[25] T. Herrmann,[51] G. Herten,[55] R. Hertenberger,[111] L. Hervas,[37] M. E. Hesping,[102] N. P. Hessey,[159a] J. Hessler,[112] M. Hidaoui,[36b] N. Hidic,[136] E. Hill,[158] S. J. Hillier,[21] J. R. Hinds,[109] F. Hinterkeuser,[25] M. Hirose,[127] S. Hirose,[160] D. Hirschbuehl,[175] T. G. Hitchings,[103] B. Hiti,[95] J. Hobbs,[149] R. Hobincu,[28e] N. Hod,[173] M. C. Hodgkinson,[143] B. H. Hodkinson,[129] A. Hoecker,[37] D. D. Hofer,[108] J. Hofer,[167] M. Holzbock,[37] L. B. A. H. Hommels,[33] B. P. Honan,[103] J. J. Hong,[69] J. Hong,[63c] T. M. Hong,[132] B. H. Hooberman,[166] W. H. Hopkins,[6] M. C. Hoppesch,[166] Y. Horii,[113] M. E. Horstmann,[112] S. Hou,[152] M. R. Housenga,[166] A. S. Howard,[95] J. Howarth,[60] J. Hoya,[6] M. Hrabovsky,[125] T. Hryn'ova,[4] P. J. Hsu,[66] S.-C. Hsu,[142] T. Hsu,[67] M. Hu,[18a] Q. Hu,[63a] S. Huang,[33] X. Huang,[14,114c] Y. Huang,[136] Y. Huang,[114b] Y. Huang,[102] Y. Huang,[14] Z. Huang,[103] Z. Hubacek,[135] M. Huebner,[25] F. Huegging,[25] T. B. Huffman,[129] M. Hufnagel Maranha De Faria,[84a] C. A. Hugli,[49] M. Huhtinen,[37] S. K. Huiberts,[17] R. Hulsken,[106] C. E. Hultquist,[18a] N. Huseynov,[12,w] J. Huston,[109] J. Huth,[62] R. Hyneman,[7] G. Iacobucci,[57] G. Iakovidis,[30] L. Iconomidou-Fayard,[67] J. P. Iddon,[37] P. Iengo,[73a,73b] R. Iguchi,[157] Y. Iiyama,[157] T. Iizawa,[129] Y. Ikegami,[85] D. Iliadis,[156] N. Ilic,[158] H. Imam,[84c] G. Inacio Goncalves,[84d] S. A. Infante Cabanas,[140c] T. Ingebretsen Carlson,[48a,48b] J. M. Inglis,[96] G. Introzzi,[74a,74b] M. Iodice,[78a] V. Ippolito,[76a,76b] R. K. Irwin,[94] M. Ishino,[157] W. Islam,[174] C. Issever,[19] S. Istin,[22a,x] H. Ito,[172] R. Iuppa,[79a,79b] A. Ivina,[173] V. Izzo,[73a] P. Jacka,[134] P. Jackson,[1] C. S. Jagfeld,[111] G. Jain,[159a] P. Jain,[49] K. Jakobs,[55] T. Jakoubek,[173] J. Jamieson,[60] W. Jang,[157] M. Javurkova,[105] P. Jawahar,[103] L. Jeanty,[126] J. Jejelava,[153a] P. Jenni,[55,y] C. E. Jessiman,[35] C. Jia,[63b] H. Jia,[168] J. Jia,[149] X. Jia,[14,114c] Z. Jia,[114a] C. Jiang,[53] Q. Jiang,[65b] S. Jiggins,[49] J. Jimenez Pena,[13] S. Jin,[114a] A. Jinaru,[28b] O. Jinnouchi,[141] P. Johansson,[143] K. A. Johns,[7] J. W. Johnson,[139] F. A. Jolly,[49] D. M. Jones,[150] E. Jones,[49] K. S. Jones,[8] P. Jones,[33] R. W. L. Jones,[93] T. J. Jones,[94] H. L. Joos,[56,37] R. Joshi,[122] J. Jovicevic,[16] X. Ju,[18a] J. J. Junggeburth,[37] T. Junkermann,[64a] A. Juste Rozas,[13,t] M. K. Juzek,[88] S. Kabana,[140e] A. Kaczmarska,[88] M. Kado,[112] H. Kagan,[122] M. Kagan,[147] A. Kahn,[131] C. Kahra,[102] T. Kaji,[157] E. Kajomovitz,[154] N. Kakati,[173] I. Kalaitzidou,[55] N. J. Kang,[139] D. Kar,[34g] K. Karava,[129] E. Karentzos,[25] O. Karkout,[117] S. N. Karpov,[40] Z. M. Karpova,[40] V. Kartvelishvili,[93] A. N. Karyukhin,[39] E. Kasimi,[156] J. Katzy,[49] S. Kaur,[35] K. Kawade,[144] M. P. Kawale,[123] C. Kawamoto,[89] T. Kawamoto,[63a] E. F. Kay,[37]

F. I. Kaya,[161] S. Kazakos,[109] V. F. Kazanin,[39] Y. Ke,[149] J. M. Keaveney,[34a] R. Keeler,[169] G. V. Kehris,[62] J. S. Keller,[35] J. J. Kempster,[150] O. Kepka,[134] J. Kerr,[159b] B. P. Kerridge,[137] B. P. Kerševan,[95] L. Keszeghova,[29a] R. A. Khan,[132] A. Khanov,[124] A. G. Kharlamov,[39] T. Kharlamova,[39] E. E. Khoda,[142] M. Kholodenko,[133a] T. J. Khoo,[19] G. Khoriauli,[170] J. Khubua,[153b,a] Y. A. R. Khwaira,[130] B. Kibirige,[34g] D. Kim,[6] D. W. Kim,[48a,48b] Y. K. Kim,[41] N. Kimura,[98] M. K. Kingston,[56] A. Kirchhoff,[56] C. Kirfel,[25] F. Kirfel,[25] J. Kirk,[137] A. E. Kiryunin,[112] S. Kita,[160] C. Kitsaki,[10] O. Kivernyk,[25] M. Klassen,[161] C. Klein,[35] L. Klein,[170] M. H. Klein,[46] S. B. Klein,[57] U. Klein,[94] P. Klimek,[37] A. Klimentov,[30] T. Klioutchnikova,[37] P. Kluit,[117] S. Kluth,[112] E. Kneringer,[80] T. M. Knight,[158] A. Knue,[50] M. Kobel,[51] D. Kobylianskii,[173] S. F. Koch,[129] M. Kocian,[147] P. Kodyš,[136] D. M. Koeck,[126] P. T. Koenig,[25] T. Koffas,[35] O. Kolay,[51] I. Koletsou,[4] T. Komarek,[88] K. Köneke,[56] A. X. Y. Kong,[1] T. Kono,[121] N. Konstantinidis,[98] P. Kontaxakis,[57] B. Konya,[100] R. Kopeliansky,[43] S. Koperny,[87a] K. Korcyl,[88] K. Kordas,[156,z] A. Korn,[98] S. Korn,[56] I. Korolkov,[13] N. Korotkova,[39] B. Kortman,[117] O. Kortner,[112] S. Kortner,[112] W. H. Kostecka,[118] V. V. Kostyukhin,[145] A. Kotsokechagia,[37] A. Kotwal,[52] A. Koulouris,[37] A. Kourkoumeli-Charalampidi,[74a,74b] C. Kourkoumelis,[9] E. Kourlitis,[112] O. Kovanda,[126] R. Kowalewski,[169] W. Kozanecki,[126] A. S. Kozhin,[39] V. A. Kramarenko,[39] G. Kramberger,[95] P. Kramer,[25] M. W. Krasny,[130] A. Krasznahorkay,[105] A. C. Kraus,[118] J. W. Kraus,[175] J. A. Kremer,[49] T. Kresse,[51] L. Kretschmann,[175] J. Kretzschmar,[94] K. Kreul,[19] P. Krieger,[158] K. Krizka,[21] K. Kroeninger,[50] H. Kroha,[112] J. Kroll,[134] J. Kroll,[131] K. S. Krowpman,[109] U. Kruchonak,[40] H. Krüger,[25] N. Krumnack,[82] M. C. Kruse,[52] O. Kuchinskaia,[39] S. Kuday,[3a] S. Kuehn,[37] R. Kuesters,[55] T. Kuhl,[49] V. Kukhtin,[40] Y. Kulchitsky,[40] S. Kuleshov,[140d,140b] M. Kumar,[34g] N. Kumari,[49] P. Kumari,[159b] A. Kupco,[134] T. Kupfer,[50] A. Kupich,[39] O. Kuprash,[55] H. Kurashige,[86] L. L. Kurchaninov,[159a] O. Kurdysh,[67] Y. A. Kurochkin,[38] A. Kurova,[39] M. Kuze,[141] A. K. Kvam,[105] J. Kvita,[125] N. G. Kyriacou,[108] L. A. O. Laatu,[104] C. Lacasta,[167] F. Lacava,[76a,76b] H. Lacker,[19] D. Lacour,[130] N. N. Lad,[98] E. Ladygin,[40] A. Lafarge,[42] B. Laforge,[130] T. Lagouri,[176] F. Z. Lahbabi,[36a] S. Lai,[56] J. E. Lambert,[169] S. Lammers,[69] W. Lampl,[7] C. Lampoudis,[156,z] G. Lamprinoudis,[102] A. N. Lancaster,[118] E. Lançon,[30] U. Landgraf,[55] M. P. J. Landon,[96] V. S. Lang,[55] O. K. B. Langrekken,[128] A. J. Lankford,[162] F. Lanni,[37] K. Lantzsch,[25] A. Lanza,[74a] M. Lanzac Berrocal,[167] J. F. Laporte,[138] T. Lari,[72a] F. Lasagni Manghi,[24b] M. Lassnig,[37] V. Latonova,[134] S. D. Lawlor,[143] Z. Lawrence,[103] R. Lazaridou,[171] M. Lazzaroni,[72a,72b] H. D. M. Le,[109] E. M. Le Boulicaut,[176] L. T. Le Pottier,[18a] B. Leban,[24b,24a] M. LeBlanc,[103] F. Ledroit-Guillon,[61] S. C. Lee,[152] T. F. Lee,[94] L. L. Leeuw,[34c,aa] M. Lefebvre,[169] C. Leggett,[18a] G. Lehmann Miotto,[37] M. Leigh,[57] W. A. Leight,[105] W. Leinonen,[116] A. Leisos,[156,bb] M. A. L. Leite,[84c] C. E. Leitgeb,[19] R. Leitner,[136] K. J. C. Leney,[46] T. Lenz,[25] S. Leone,[75a] C. Leonidopoulos,[53] A. Leopold,[148] J. H. Lepage Bourbonnais,[35] R. Les,[109] C. G. Lester,[33] M. Levchenko,[39] J. Levêque,[4] L. J. Levinson,[173] G. Levrini,[24b,24a] M. P. Lewicki,[88] C. Lewis,[142] D. J. Lewis,[4] L. Lewitt,[143] A. Li,[30] B. Li,[63b] C. Li,[108] C-Q. Li,[112] H. Li,[63a] H. Li,[63b] H. Li,[114a] H. Li,[15] H. Li,[63a] H. Li,[63b] J. Li,[63c] K. Li,[14] L. Li,[63c] R. Li,[176] S. Li,[14,114c] S. Li,[63d,63c,cc] T. Li,[5] X. Li,[106] Z. Li,[157] Z. Li,[14,114c] Z. Li,[63a] S. Liang,[14,114c] Z. Liang,[14] M. Liberatore,[138] B. Liberti,[77a] K. Lie,[65c] J. Lieber Marin,[84e] H. Lien,[69] H. Lin,[108] L. Linden,[111] R. E. Lindley,[7] J. H. Lindon,[2] J. Ling,[62] E. Lipeles,[131] A. Lipniacka,[17] A. Lister,[168] J. D. Little,[69] B. Liu,[14] B. X. Liu,[114b] D. Liu,[63d,63c] E. H. L. Liu,[21] J. K. K. Liu,[33] K. Liu,[63d] K. Liu,[63d,63c] M. Liu,[63a] M. Y. Liu,[63a] P. Liu,[14] Q. Liu,[63d,142,63c] X. Liu,[63a] X. Liu,[63b] Y. Liu,[114b,114c] Y. L. Liu,[63b] Y. W. Liu,[63a] S. L. Lloyd,[96] E. M. Lobodzinska,[49] P. Loch,[7] E. Lodhi,[158] T. Lohse,[19] K. Lohwasser,[143] E. Loiacono,[49] J. D. Lomas,[21] J. D. Long,[43] I. Longarini,[162] R. Longo,[166] A. Lopez Solis,[49] N. A. Lopez-canelas,[7] N. Lorenzo Martinez,[4] A. M. Lory,[111] M. Losada,[119a] G. Löschcke Centeno,[150] O. Loseva,[39] X. Lou,[48a,48b] X. Lou,[14,114c] A. Lounis,[67] P. A. Love,[93] G. Lu,[14,114c] M. Lu,[67] S. Lu,[131] Y. J. Lu,[152] H. J. Lubatti,[142] C. Luci,[76a,76b] F. L. Lucio Alves,[114a] F. Luehring,[69] O. Lukianchuk,[67] B. S. Lunday,[131] O. Lundberg,[148] B. Lund-Jensen,[148,a] N. A. Luongo,[6] M. S. Lutz,[37] A. B. Lux,[26] D. Lynn,[30] R. Lysak,[134] E. Lytken,[100] V. Lyubushkin,[40] T. Lyubushkina,[40] M. M. Lyukova,[149] M. Firdaus M. Soberi,[53] H. Ma,[30] K. Ma,[63a] L. L. Ma,[63b] W. Ma,[63a] Y. Ma,[124] J. C. MacDonald,[102] P. C. Machado De Abreu Farias,[84e] R. Madar,[42] T. Madula,[98] J. Maeda,[86] T. Maeno,[30] P. T. Mafa,[34c,dd] H. Maguire,[143] V. Maiboroda,[138] A. Maio,[133a,133b,133d] K. Maj,[87a] O. Majersky,[49] S. Majewski,[126] R. Makhmanazarov,[39] N. Makovec,[67] V. Maksimovic,[16] B. Malaescu,[130] Pa. Malecki,[88] V. P. Maleev,[39] F. Malek,[61,ee] M. Mali,[95] D. Malito,[97] U. Mallik,[81,a]

S. Maltezos,[10] S. Malyukov,[40] J. Mamuzic,[13] G. Mancini,[54] M. N. Mancini,[27] G. Manco,[74a,74b] J. P. Mandalia,[96] S. S. Mandarry,[150] I. Mandić,[95] L. Manhaes de Andrade Filho,[84a] I. M. Maniatis,[173] J. Manjarres Ramos,[91] D. C. Mankad,[173] A. Mann,[111] S. Manzoni,[37] L. Mao,[63c] X. Mapekula,[34c] A. Marantis,[156,bb] G. Marchiori,[5] M. Marcisovsky,[134] C. Marcon,[72a] M. Marinescu,[21] S. Marium,[49] M. Marjanovic,[123] A. Markhoos,[55] M. Markovitch,[67] M. K. Maroun,[105] E. J. Marshall,[93] Z. Marshall,[18a] S. Marti-Garcia,[167] J. Martin,[98] T. A. Martin,[137] V. J. Martin,[53] B. Martin dit Latour,[17] L. Martinelli,[76a,76b] M. Martinez,[13,t] P. Martinez Agullo,[167] V. I. Martinez Outschoorn,[105] P. Martinez Suarez,[13] S. Martin-Haugh,[137] G. Martinovicova,[136] V. S. Martoiu,[28b] A. C. Martyniuk,[98] A. Marzin,[37] D. Mascione,[79a,79b] L. Masetti,[102] J. Masik,[103] A. L. Maslennikov,[39] S. L. Mason,[43] P. Massarotti,[73a,73b] P. Mastrandrea,[75a,75b] A. Mastroberardino,[45b,45a] T. Masubuchi,[127] T. T. Mathew,[126] J. Matousek,[136] D. M. Mattern,[50] J. Maurer,[28b] T. Maurin,[60] A. J. Maury,[67] B. Maček,[95] D. A. Maximov,[39] A. E. May,[103] R. Mazini,[34g] I. Maznas,[118] M. Mazza,[109] S. M. Mazza,[139] E. Mazzeo,[72a,72b] J. P. Mc Gowan,[169] S. P. Mc Kee,[108] C. A. Mc Lean,[6] C. C. McCracken,[168] E. F. McDonald,[107] A. E. McDougall,[117] L. F. Mcelhinney,[93] J. A. Mcfayden,[150] R. P. McGovern,[131] R. P. Mckenzie,[34g] T. C. Mclachlan,[49] D. J. Mclaughlin,[98] S. J. McMahon,[137] C. M. Mcpartland,[94] R. A. McPherson,[169,o] S. Mehlhase,[111] A. Mehta,[94] D. Melini,[167] B. R. Mellado Garcia,[34g] A. H. Melo,[56] F. Meloni,[49] A. M. Mendes Jacques Da Costa,[103] H. Y. Meng,[158] L. Meng,[93] S. Menke,[112] M. Mentink,[37] E. Meoni,[45b,45a] G. Mercado,[118] S. Merianos,[156] C. Merlassino,[70a,70c] C. Meroni,[72a,72b] J. Metcalfe,[6] A. S. Mete,[6] E. Meuser,[102] C. Meyer,[69] J-P. Meyer,[138] R. P. Middleton,[137] L. Mijović,[53] G. Mikenberg,[173] M. Mikestikova,[134] M. Mikuž,[95] H. Mildner,[102] A. Milic,[37] D. W. Miller,[41] E. H. Miller,[147] L. S. Miller,[35] A. Milov,[173] D. A. Milstead,[48a,48b] T. Min,[114a] A. A. Minaenko,[39] I. A. Minashvili,[153b] A. I. Mincer,[120] B. Mindur,[87a] M. Mineev,[40] Y. Mino,[89] L. M. Mir,[13] M. Miralles Lopez,[60] M. Mironova,[18a] M. C. Missio,[116] A. Mitra,[171] V. A. Mitsou,[167] Y. Mitsumori,[113] O. Miu,[158] P. S. Miyagawa,[96] T. Mkrtchyan,[64a] M. Mlinarevic,[98] T. Mlinarevic,[98] M. Mlynarikova,[37] S. Mobius,[20] P. Mogg,[111] M. H. Mohamed Farook,[115] A. F. Mohammed,[14,114c] S. Mohapatra,[43] G. Mokgatitswane,[34g] L. Moleri,[173] B. Mondal,[145] S. Mondal,[135] K. Mönig,[49] E. Monnier,[104] L. Monsonis Romero,[167] J. Montejo Berlingen,[13] A. Montella,[48a,48b] M. Montella,[122] F. Montereali,[78a,78b] F. Monticelli,[92] S. Monzani,[70a,70c] A. Morancho Tarda,[44] N. Morange,[67] A. L. Moreira De Carvalho,[49] M. Moreno Llácer,[167] C. Moreno Martinez,[57] J. M. Moreno Perez,[23b] P. Morettini,[58b] S. Morgenstern,[37] M. Morii,[62] M. Morinaga,[157] M. Moritsu,[90] F. Morodei,[76a,76b] P. Moschovakos,[37] B. Moser,[129] M. Mosidze,[153b] T. Moskalets,[46] P. Moskvitina,[116] J. Moss,[32,ff] P. Moszkowicz,[87a] A. Moussa,[36d] Y. Moyal,[173] E. J. W. Moyse,[105] O. Mtintsilana,[34g] S. Muanza,[104] J. Mueller,[132] D. Muenstermann,[93] R. Müller,[37] G. A. Mullier,[165] A. J. Mullin,[33] J. J. Mullin,[131] A. E. Mulski,[62] D. P. Mungo,[158] D. Munoz Perez,[167] F. J. Munoz Sanchez,[103] M. Murin,[103] W. J. Murray,[171,137] M. Muškinja,[95] C. Mwewa,[30] A. G. Myagkov,[39,k] A. J. Myers,[8] G. Myers,[108] M. Myska,[135] B. P. Nachman,[18a] K. Nagai,[129] K. Nagano,[85] R. Nagasaka,[157] J. L. Nagle,[30,gg] E. Nagy,[104] A. M. Nairz,[37] Y. Nakahama,[85] K. Nakamura,[85] K. Nakkalil,[5] H. Nanjo,[127] E. A. Narayanan,[46] Y. Narukawa,[157] I. Naryshkin,[39] L. Nasella,[72a,72b] S. Nasri,[119b] C. Nass,[25] G. Navarro,[23a] J. Navarro-Gonzalez,[167] A. Nayaz,[19] P. Y. Nechaeva,[39] S. Nechaeva,[24b,24a] F. Nechansky,[134] L. Nedic,[129] T. J. Neep,[21] A. Negri,[74a,74b] M. Negrini,[24b] C. Nellist,[117] C. Nelson,[106] K. Nelson,[108] S. Nemecek,[134] M. Nessi,[37,hh] M. S. Neubauer,[166] F. Neuhaus,[102] J. Newell,[94] P. R. Newman,[21] Y. W. Y. Ng,[166] B. Ngair,[119a] H. D. N. Nguyen,[110] R. B. Nickerson,[129] R. Nicolaidou,[138] J. Nielsen,[139] M. Niemeyer,[56] J. Niermann,[37] N. Nikiforou,[37] V. Nikolaenko,[39,k] I. Nikolic-Audit,[130] P. Nilsson,[30] I. Ninca,[49] G. Ninio,[155] A. Nisati,[76a] N. Nishu,[2] R. Nisius,[112] N. Nitika,[70a,70c] J-E. Nitschke,[51] E. K. Nkadimeng,[34g] T. Nobe,[157] T. Nommensen,[151] M. B. Norfolk,[143] B. J. Norman,[35] M. Noury,[36a] J. Novak,[95] T. Novak,[95] R. Novotny,[115] L. Nozka,[125] K. Ntekas,[162] N. M. J. Nunes De Moura Junior,[84b] J. Ocariz,[130] A. Ochi,[86] I. Ochoa,[133a] S. Oerdek,[49,ii] J. T. Offermann,[41] A. Ogrodnik,[136] A. Oh,[103] C. C. Ohm,[148] H. Oide,[85] R. Oishi,[157] M. L. Ojeda,[37] Y. Okumura,[157] L. F. Oleiro Seabra,[133a] I. Oleksiyuk,[57] S. A. Olivares Pino,[140d] G. Oliveira Correa,[13] D. Oliveira Damazio,[30] J. L. Oliver,[162] Ö. O. Öncel,[55] A. P. O'Neill,[20] A. Onofre,[133a,133e] P. U. E. Onyisi,[11] M. J. Oreglia,[41] D. Orestano,[78a,78b] R. S. Orr,[158] L. M. Osojnak,[131] Y. Osumi,[113] G. Otero y Garzon,[31] H. Otono,[90] P. S. Ott,[64a] G. J. Ottino,[18a] M. Ouchrif,[36d] F. Ould-Saada,[128] T. Ovsiannikova,[142] M. Owen,[60] R. E. Owen,[137] V. E. Ozcan,[22a] F. Ozturk,[88] N. Ozturk,[8] S. Ozturk,[83] H. A. Pacey,[129] K. Pachal,[159a] A. Pacheco Pages,[13] C. Padilla Aranda,[13] G. Padovano,[76a,76b]

S. Pagan Griso,[18a] G. Palacino,[69] A. Palazzo,[71a,71b] J. Pampel,[25] J. Pan,[176] T. Pan,[65a] D. K. Panchal,[11] C. E. Pandini,[117] J. G. Panduro Vazquez,[137] H. D. Pandya,[1] H. Pang,[138] P. Pani,[49] G. Panizzo,[70a,70c] L. Panwar,[130] L. Paolozzi,[57] S. Parajuli,[166] A. Paramonov,[6] C. Paraskevopoulos,[54] D. Paredes Hernandez,[65b] A. Pareti,[74a,74b] K. R. Park,[43] T. H. Park,[112] F. Parodi,[58b,58a] E. W. Parrish,[118] J. A. Parsons,[43] U. Parzefall,[55] B. Pascual Dias,[110] L. Pascual Dominguez,[101] E. Pasqualucci,[76a] S. Passaggio,[58b] F. Pastore,[97] P. Patel,[88] U. M. Patel,[52] J. R. Pater,[103] T. Pauly,[37] F. Pauwels,[136] C. I. Pazos,[161] M. Pedersen,[128] R. Pedro,[133a] S. V. Peleganchuk,[39] O. Penc,[37] E. A. Pender,[53] S. Peng,[15] G. D. Penn,[176] K. E. Penski,[111] M. Penzin,[39] B. S. Peralva,[84d] A. P. Pereira Peixoto,[142] L. Pereira Sanchez,[147] D. V. Perepelitsa,[30,gg] G. Perera,[105] E. Perez Codina,[159a] M. Perganti,[10] H. Pernegger,[37] S. Perrella,[76a,76b] O. Perrin,[42] K. Peters,[49] R. F. Y. Peters,[103] B. A. Petersen,[37] T. C. Petersen,[44] E. Petit,[104] V. Petousis,[135] C. Petridou,[156,z] T. Petru,[136] A. Petrukhin,[145] M. Pettee,[18a] A. Petukhov,[83] K. Petukhova,[37] R. Pezoa,[140f] L. Pezzotti,[37] G. Pezzullo,[176] A. J. Pfleger,[37] T. M. Pham,[174] T. Pham,[107] P. W. Phillips,[137] G. Piacquadio,[149] E. Pianori,[18a] F. Piazza,[126] R. Piegaia,[31] D. Pietreanu,[28b] A. D. Pilkington,[103] M. Pinamonti,[70a,70c] J. L. Pinfold,[2] B. C. Pinheiro Pereira,[133a] J. Pinol Bel,[13] A. E. Pinto Pinoargote,[138] L. Pintucci,[70a,70c] K. M. Piper,[150] A. Pirttikoski,[57] D. A. Pizzi,[35] L. Pizzimento,[65b] M.-A. Pleier,[30] V. Pleskot,[136] E. Plotnikova,[40] G. Poddar,[96] R. Poettgen,[100] L. Poggioli,[130] S. Polacek,[136] G. Polesello,[74a] A. Poley,[146,159a] A. Polini,[24b] C. S. Pollard,[171] Z. B. Pollock,[122] E. Pompa Pacchi,[123] N. I. Pond,[98] D. Ponomarenko,[69] L. Pontecorvo,[37] S. Popa,[28a] G. A. Popeneciu,[28d] A. Poreba,[37] D. M. Portillo Quintero,[159a] S. Pospisil,[135] M. A. Postill,[143] P. Postolache,[28c] K. Potamianos,[171] P. A. Potepa,[87a] I. N. Potrap,[40] C. J. Potter,[33] H. Potti,[151] J. Poveda,[167] M. E. Pozo Astigarraga,[37] A. Prades Ibanez,[77a,77b] J. Pretel,[169] D. Price,[103] M. Primavera,[71a] L. Primomo,[70a,70c] M. A. Principe Martin,[101] R. Privara,[125] T. Procter,[60] M. L. Proffitt,[142] N. Proklova,[131] K. Prokofiev,[65c] G. Proto,[112] J. Proudfoot,[6] M. Przybycien,[87a] W. W. Przygoda,[87b] A. Psallidas,[47] J. E. Puddefoot,[143] D. Pudzha,[55] D. Pyatiizbyantseva,[116] J. Qian,[108] R. Qian,[109] D. Qichen,[103] Y. Qin,[13] T. Qiu,[53] A. Quadt,[56] M. Queitsch-Maitland,[103] G. Quetant,[57] R. P. Quinn,[168] G. Rabanal Bolanos,[62] D. Rafanoharana,[55] F. Raffaeli,[77a,77b] F. Ragusa,[72a,72b] J. L. Rainbolt,[41] J. A. Raine,[57] S. Rajagopalan,[30] E. Ramakoti,[39] L. Rambelli,[58b,58a] I. A. Ramirez-Berend,[35] K. Ran,[49,114c] D. S. Rankin,[131] N. P. Rapheeha,[34g] H. Rasheed,[28b] V. Raskina,[130] D. F. Rassloff,[64a] A. Rastogi,[18a] S. Rave,[102] S. Ravera,[58b,58a] B. Ravina,[37] I. Ravinovich,[173] M. Raymond,[37] A. L. Read,[128] N. P. Readioff,[143] D. M. Rebuzzi,[74a,74b] A. S. Reed,[112] K. Reeves,[27] J. A. Reidelsturz,[175] D. Reikher,[126] A. Rej,[50] C. Rembser,[37] H. Ren,[63a] M. Renda,[28b] F. Renner,[49] A. G. Rennie,[162] A. L. Rescia,[49] S. Resconi,[72a] M. Ressegotti,[58b,58a] S. Rettie,[37] W. F. Rettie,[35] J. G. Reyes Rivera,[109] E. Reynolds,[18a] O. L. Rezanova,[39] P. Reznicek,[136] H. Riani,[36d] N. Ribaric,[52] E. Ricci,[79a,79b] R. Richter,[112] S. Richter,[48a,48b] E. Richter-Was,[87b] M. Ridel,[130] S. Ridouani,[36d] P. Rieck,[120] P. Riedler,[37] E. M. Riefel,[48a,48b] J. O. Rieger,[117] M. Rijssenbeek,[149] M. Rimoldi,[37] L. Rinaldi,[24b,24a] P. Rincke,[56] M. P. Rinnagel,[111] G. Ripellino,[165] I. Riu,[13] J. C. Rivera Vergara,[169] F. Rizatdinova,[124] E. Rizvi,[96] B. R. Roberts,[18a] S. S. Roberts,[139] D. Robinson,[33] M. Robles Manzano,[102] A. Robson,[60] A. Rocchi,[77a,77b] C. Roda,[75a,75b] S. Rodriguez Bosca,[37] Y. Rodriguez Garcia,[23a] A. M. Rodríguez Vera,[118] S. Roe,[37] J. T. Roemer,[37] O. Røhne,[128] R. A. Rojas,[37] C. P. A. Roland,[130] J. Roloff,[30] A. Romaniouk,[80] E. Romano,[74a,74b] M. Romano,[24b] A. C. Romero Hernandez,[166] N. Rompotis,[94] L. Roos,[130] S. Rosati,[76a] B. J. Rosser,[41] E. Rossi,[129] E. Rossi,[73a,73b] L. P. Rossi,[62] L. Rossini,[55] R. Rosten,[122] M. Rotaru,[28b] B. Rottler,[55] C. Rougier,[91] D. Rousseau,[67] D. Rousso,[49] S. Roy-Garand,[158] A. Rozanov,[104] Z. M. A. Rozario,[60] Y. Rozen,[154] A. Rubio Jimenez,[167] V. H. Ruelas Rivera,[19] T. A. Ruggeri,[1] A. Ruggiero,[129] A. Ruiz-Martinez,[167] A. Rummler,[37] Z. Rurikova,[55] N. A. Rusakovich,[40] H. L. Russell,[169] G. Russo,[76a,76b] J. P. Rutherfoord,[7] S. Rutherford Colmenares,[33] M. Rybar,[136] E. B. Rye,[128] A. Ryzhov,[46] J. A. Sabater Iglesias,[57] H. F-W. Sadrozinski,[139] F. Safai Tehrani,[76a] S. Saha,[1] M. Sahinsoy,[83] A. Saibel,[167] M. Saimpert,[138] M. Saito,[157] T. Saito,[157] A. Sala,[72a,72b] D. Salamani,[37] A. Salnikov,[147] J. Salt,[167] A. Salvador Salas,[155] D. Salvatore,[45b,45a] F. Salvatore,[150] A. Salzburger,[37] D. Sammel,[55] E. Sampson,[93] D. Sampsonidis,[156,z] D. Sampsonidou,[126] J. Sánchez,[167] V. Sanchez Sebastian,[167] H. Sandaker,[128] C. O. Sander,[49] J. A. Sandesara,[105] M. Sandhoff,[175] C. Sandoval,[23b] L. Sanfilippo,[64a] D. P. C. Sankey,[137] T. Sano,[89] A. Sansoni,[54] L. Santi,[37,76b] C. Santoni,[42] H. Santos,[133a,133b] A. Santra,[173] E. Sanzani,[24b,24a] K. A. Saoucha,[164] J. G. Saraiva,[133a,133d] J. Sardain,[7] O. Sasaki,[85] K. Sato,[160] C. Sauer,[37] E. Sauvan,[4] P. Savard,[158,e] R. Sawada,[157] C. Sawyer,[137] L. Sawyer,[99] C. Sbarra,[24b] A. Sbrizzi,[24b,24a]

T. Scanlon,[98] J. Schaarschmidt,[142] U. Schäfer,[102] A. C. Schaffer,[67,46] D. Schaile,[111] R. D. Schamberger,[149] C. Scharf,[19] M. M. Schefer,[20] V. A. Schegelsky,[39] D. Scheirich,[136] M. Schernau,[140e] C. Scheulen,[57] C. Schiavi,[58b,58a] M. Schioppa,[45b,45a] B. Schlag,[147] S. Schlenker,[37] J. Schmeing,[175] M. A. Schmidt,[175] K. Schmieden,[102] C. Schmitt,[102] N. Schmitt,[102] S. Schmitt,[49] L. Schoeffel,[138] A. Schoening,[64b] P. G. Scholer,[35] E. Schopf,[129] M. Schott,[25] J. Schovancova,[37] S. Schramm,[57] T. Schroer,[57] H-C. Schultz-Coulon,[64a] M. Schumacher,[55] B. A. Schumm,[139] Ph. Schune,[138] H. R. Schwartz,[139] A. Schwartzman,[147] T. A. Schwarz,[108] Ph. Schwemling,[138] R. Schwienhorst,[109] F. G. Sciacca,[20] A. Sciandra,[30] G. Sciolla,[27] F. Scuri,[75a] C. D. Sebastiani,[94] K. Sedlaczek,[118] S. C. Seidel,[115] A. Seiden,[139] B. D. Seidlitz,[43] C. Seitz,[49] J. M. Seixas,[84b] G. Sekhniaidze,[73a] L. Selem,[61] N. Semprini-Cesari,[24b,24a] A. Semushin,[177,39] D. Sengupta,[57] V. Senthilkumar,[167] L. Serin,[67] M. Sessa,[77a,77b] H. Severini,[123] F. Sforza,[58b,58a] A. Sfyrla,[57] Q. Sha,[14] E. Shabalina,[56] H. Shaddix,[118] A. H. Shah,[33] R. Shaheen,[148] J. D. Shahinian,[131] D. Shaked Renous,[173] L. Y. Shan,[14] M. Shapiro,[18a] A. Sharma,[37] A. S. Sharma,[168] P. Sharma,[30] P. B. Shatalov,[39] K. Shaw,[150] S. M. Shaw,[103] Q. Shen,[63c] D. J. Sheppard,[146] P. Sherwood,[98] L. Shi,[98] X. Shi,[14] S. Shimizu,[85] C. O. Shimmin,[176] I. P. J. Shipsey,[129,a] S. Shirabe,[90] A. R. Shirazi-Nejad,[8] M. Shiyakova,[40,jj] M. J. Shochet,[41] D. R. Shope,[128] B. Shrestha,[123] S. Shrestha,[122,kk] I. Shreyber,[39] M. J. Shroff,[169] P. Sicho,[134] A. M. Sickles,[166] E. Sideras Haddad,[34g,163] A. C. Sidley,[117] A. Sidoti,[24b] F. Siegert,[51] Dj. Sijacki,[16] F. Sili,[92] J. M. Silva,[53] I. Silva Ferreira,[84b] M. V. Silva Oliveira,[30] S. B. Silverstein,[48a] S. Simion,[67] R. Simoniello,[37] E. L. Simpson,[103] H. Simpson,[150] L. R. Simpson,[108] S. Simsek,[83] S. Sindhu,[56] P. Sinervo,[158] S. N. Singh,[27] S. Singh,[30] S. Sinha,[49] S. Sinha,[103] M. Sioli,[24b,24a] K. Sioulas,[9] I. Siral,[37] E. Sitnikova,[49] J. Sjölin,[48a,48b] A. Skaf,[56] E. Skorda,[21] P. Skubic,[123] M. Slawinska,[88] I. Slazyk,[17] V. Smakhtin,[173] B. H. Smart,[137] S. Yu. Smirnov,[39] Y. Smirnov,[39] L. N. Smirnova,[39,k] O. Smirnova,[100] A. C. Smith,[43] D. R. Smith,[162] E. A. Smith,[41] J. L. Smith,[103] M. B. Smith,[35] R. Smith,[147] H. Smitmanns,[102] M. Smizanska,[93] K. Smolek,[135] A. A. Snesarev,[39] H. L. Snoek,[117] S. Snyder,[30] R. Sobie,[169,o] A. Soffer,[155] C. A. Solans Sanchez,[37] E. Yu. Soldatov,[39] U. Soldevila,[167] A. A. Solodkov,[39] S. Solomon,[27] A. Soloshenko,[40] K. Solovieva,[55] O. V. Solovyanov,[42] P. Sommer,[51] A. Sonay,[13] W. Y. Song,[159b] A. Sopczak,[135] A. L. Sopio,[53] F. Sopkova,[29b] J. D. Sorenson,[115] I. R. Sotarriva Alvarez,[141] V. Sothilingam,[64a] O. J. Soto Sandoval,[140c,140b] S. Sottocornola,[69] R. Soualah,[164] Z. Soumaimi,[36e] D. South,[49] N. Soybelman,[173] S. Spagnolo,[71a,71b] M. Spalla,[112] D. Sperlich,[55] B. Spisso,[73a,73b] D. P. Spiteri,[60] M. Spousta,[136] E. J. Staats,[35] R. Stamen,[64a] E. Stanecka,[88] W. Stanek-Maslouska,[49] M. V. Stange,[51] B. Stanislaus,[18a] M. M. Stanitzki,[49] B. Stapf,[49] E. A. Starchenko,[39] G. H. Stark,[139] J. Stark,[91] P. Staroba,[134] P. Starovoitov,[164] R. Staszewski,[88] G. Stavropoulos,[47] A. Stefl,[37] P. Steinberg,[30] B. Stelzer,[146,159a] H. J. Stelzer,[132] O. Stelzer-Chilton,[159a] H. Stenzel,[59] T. J. Stevenson,[150] G. A. Stewart,[37] J. R. Stewart,[124] M. C. Stockton,[37] G. Stoicea,[28b] M. Stolarski,[133a] S. Stonjek,[112] A. Straessner,[51] J. Strandberg,[148] S. Strandberg,[48a,48b] M. Stratmann,[175] M. Strauss,[123] T. Strebler,[104] P. Strizenec,[29b] R. Ströhmer,[170] D. M. Strom,[126] R. Stroynowski,[46] A. Strubig,[48a,48b] S. A. Stucci,[30] B. Stugu,[17] J. Stupak,[123] N. A. Styles,[49] D. Su,[147] S. Su,[63a] W. Su,[63d] X. Su,[63a] D. Suchy,[29a] K. Sugizaki,[131] V. V. Sulin,[39] M. J. Sullivan,[94] D. M. S. Sultan,[129] L. Sultanaliyeva,[39] S. Sultansoy,[3b] S. Sun,[174] W. Sun,[14] O. Sunneborn Gudnadottir,[165] N. Sur,[104] M. R. Sutton,[150] H. Suzuki,[160] M. Svatos,[134] M. Swiatlowski,[159a] T. Swirski,[170] I. Sykora,[29a] M. Sykora,[136] T. Sykora,[136] D. Ta,[102] K. Tackmann,[49,ii] A. Taffard,[162] R. Tafirout,[159a] J. S. Tafoya Vargas,[67] Y. Takubo,[85] M. Talby,[104] A. A. Talyshev,[39] K. C. Tam,[65b] N. M. Tamir,[155] A. Tanaka,[157] J. Tanaka,[157] R. Tanaka,[67] M. Tanasini,[149] Z. Tao,[168] S. Tapia Araya,[140f] S. Tapprogge,[102] A. Tarek Abouelfadl Mohamed,[109] S. Tarem,[154] K. Tariq,[14] G. Tarna,[28b] G. F. Tartarelli,[72a] M. J. Tartarin,[91] P. Tas,[136] M. Tasevsky,[134] E. Tassi,[45b,45a] A. C. Tate,[166] G. Tateno,[157] Y. Tayalati,[36e,ll] G. N. Taylor,[107] W. Taylor,[159b] P. Teixeira-Dias,[97] J. J. Teoh,[158] K. Terashi,[157] J. Terron,[101] S. Terzo,[13] M. Testa,[54] R. J. Teuscher,[158,o] A. Thaler,[80] O. Theiner,[57] T. Theveneaux-Pelzer,[104] O. Thielmann,[175] D. W. Thomas,[97] J. P. Thomas,[21] E. A. Thompson,[18a] P. D. Thompson,[21] E. Thomson,[131] R. E. Thornberry,[46] C. Tian,[63a] Y. Tian,[57] V. Tikhomirov,[39,k] Yu. A. Tikhonov,[39] S. Timoshenko,[39] D. Timoshyn,[136] E. X. L. Ting,[1] P. Tipton,[176] A. Tishelman-Charny,[30] S. H. Tlou,[34g] K. Todome,[141] S. Todorova-Nova,[136] S. Todt,[51] L. Toffolin,[70a,70c] M. Togawa,[85] J. Tojo,[90] S. Tokár,[29a] O. Toldaiev,[69] G. Tolkachev,[104] M. Tomoto,[85,113] L. Tompkins,[147,mm] E. Torrence,[126] H. Torres,[91] E. Torró Pastor,[167] M. Toscani,[31] C. Tosciri,[41] M. Tost,[11] D. R. Tovey,[143] T. Trefzger,[170] A. Tricoli,[30] I. M. Trigger,[159a]

S. Trincaz-Duvoid,[130] D. A. Trischuk,[27] A. Tropina,[40] L. Truong,[34c] M. Trzebinski,[88] A. Trzupek,[88] F. Tsai,[149] M. Tsai,[108] A. Tsiamis,[156] P. V. Tsiareshka,[40] S. Tsigaridas,[159a] A. Tsirigotis,[156,bb] V. Tsiskaridze,[158] E. G. Tskhadadze,[153a] M. Tsopoulou,[156] Y. Tsujikawa,[89] I. I. Tsukerman,[39] V. Tsulaia,[18a] S. Tsuno,[85] K. Tsuri,[121] D. Tsybychev,[149] Y. Tu,[65b] A. Tudorache,[28b] V. Tudorache,[28b] S. Turchikhin,[58b,58a] I. Turk Cakir,[3a] R. Turra,[72a] T. Turtuvshin,[40,nn] P. M. Tuts,[43] S. Tzamarias,[156,z] E. Tzovara,[102] F. Ukegawa,[160] P. A. Ulloa Poblete,[140c,140b] E. N. Umaka,[30] G. Unal,[37] A. Undrus,[30] G. Unel,[162] J. Urban,[29b] P. Urrejola,[140a] G. Usai,[8] R. Ushioda,[141] M. Usman,[110] F. Ustuner,[53] Z. Uysal,[83] V. Vacek,[135] B. Vachon,[106] T. Vafeiadis,[37] A. Vaitkus,[98] C. Valderanis,[111] E. Valdes Santurio,[48a,48b] M. Valente,[159a] S. Valentinetti,[24b,24a] A. Valero,[167] E. Valiente Moreno,[167] A. Vallier,[91] J. A. Valls Ferrer,[167] D. R. Van Arneman,[117] T. R. Van Daalen,[142] A. Van Der Graaf,[50] P. Van Gemmeren,[6] M. Van Rijnbach,[37] S. Van Stroud,[98] I. Van Vulpen,[117] P. Vana,[136] M. Vanadia,[77a,77b] U. M. Vande Voorde,[148] W. Vandelli,[37] E. R. Vandewall,[124] D. Vannicola,[155] L. Vannoli,[54] R. Vari,[76a] E. W. Varnes,[7] C. Varni,[18b] D. Varouchas,[67] L. Varriale,[167] K. E. Varvell,[151] M. E. Vasile,[28b] L. Vaslin,[85] A. Vasyukov,[40] L. M. Vaughan,[124] R. Vavricka,[102] T. Vazquez Schroeder,[13] J. Veatch,[32] V. Vecchio,[103] M. J. Veen,[105] I. Veliscek,[30] L. M. Veloce,[158] F. Veloso,[133a,133c] S. Veneziano,[76a] A. Ventura,[71a,71b] S. Ventura Gonzalez,[138] A. Verbytskyi,[112] M. Verducci,[75a,75b] C. Vergis,[96] M. Verissimo De Araujo,[84b] W. Verkerke,[117] J. C. Vermeulen,[117] C. Vernieri,[147] M. Vessella,[162] M. C. Vetterli,[146,e] A. Vgenopoulos,[102] N. Viaux Maira,[140f] T. Vickey,[143] O. E. Vickey Boeriu,[143] G. H. A. Viehhauser,[129] L. Vigani,[64b] M. Vigl,[112] M. Villa,[24b,24a] M. Villaplana Perez,[167] E. M. Villhauer,[53] E. Vilucchi,[54] M. G. Vincter,[35] A. Visibile,[117] C. Vittori,[37] I. Vivarelli,[24b,24a] E. Voevodina,[112] F. Vogel,[111] J. C. Voigt,[51] P. Vokac,[135] Yu. Volkotrub,[87b] E. Von Toerne,[25] B. Vormwald,[37] K. Vorobev,[39] M. Vos,[167] K. Voss,[145] M. Vozak,[117] L. Vozdecky,[123] N. Vranjes,[16] M. Vranjes Milosavljevic,[16] M. Vreeswijk,[117] N. K. Vu,[63d,63c] R. Vuillermet,[37] O. Vujinovic,[102] I. Vukotic,[41] I. K. Vyas,[35] S. Wada,[160] C. Wagner,[147] J. M. Wagner,[18a] W. Wagner,[175] S. Wahdan,[175] H. Wahlberg,[92] C. H. Waits,[123] J. Walder,[137] R. Walker,[111] W. Walkowiak,[145] A. Wall,[131] E. J. Wallin,[100] T. Wamorkar,[18a] A. Z. Wang,[139] C. Wang,[102] C. Wang,[11] H. Wang,[18a] J. Wang,[65c] P. Wang,[103] P. Wang,[98] R. Wang,[62] R. Wang,[6] S. M. Wang,[152] S. Wang,[14] T. Wang,[63a] W. T. Wang,[81] W. Wang,[14] X. Wang,[166] X. Wang,[63c] Y. Wang,[114a] Y. Wang,[63a] Z. Wang,[108] Z. Wang,[63d,52,63c] Z. Wang,[108] C. Wanotayaroj,[85] A. Warburton,[106] R. J. Ward,[21] A. L. Warnerbring,[145] N. Warrack,[60] S. Waterhouse,[97] A. T. Watson,[21] H. Watson,[53] M. F. Watson,[21] E. Watton,[60,137] G. Watts,[142] B. M. Waugh,[98] J. M. Webb,[55] C. Weber,[30] H. A. Weber,[19] M. S. Weber,[20] S. M. Weber,[64a] C. Wei,[63a] Y. Wei,[55] A. R. Weidberg,[129] E. J. Weik,[120] J. Weingarten,[50] C. Weiser,[55] C. J. Wells,[49] T. Wenaus,[30] B. Wendland,[50] T. Wengler,[37] N. S. Wenke,[112] N. Wermes,[25] M. Wessels,[64a] A. M. Wharton,[93] A. S. White,[62] A. White,[8] M. J. White,[1] D. Whiteson,[162] L. Wickremasinghe,[127] W. Wiedenmann,[174] M. Wielers,[137] C. Wiglesworth,[44] D. J. Wilbern,[123] H. G. Wilkens,[37] J. J. H. Wilkinson,[33] D. M. Williams,[43] H. H. Williams,[131] S. Williams,[33] S. Willocq,[105] B. J. Wilson,[103] D. J. Wilson,[103] P. J. Windischhofer,[41] F. I. Winkel,[31] F. Winklmeier,[126] B. T. Winter,[55] M. Wittgen,[147] M. Wobisch,[99] T. Wojtkowski,[61] Z. Wolffs,[117] J. Wollrath,[37] M. W. Wolter,[88] H. Wolters,[133a,133c] M. C. Wong,[139] E. L. Woodward,[43] S. D. Worm,[49] B. K. Wosiek,[88] K. W. Woźniak,[88] S. Wozniewski,[56] K. Wraight,[60] C. Wu,[21] M. Wu,[114b] M. Wu,[116] S. L. Wu,[174] X. Wu,[57] X. Wu,[63a] Y. Wu,[63a] Z. Wu,[4] J. Wuerzinger,[112,v] T. R. Wyatt,[103] B. M. Wynne,[53] S. Xella,[44] L. Xia,[114a] M. Xia,[15] M. Xie,[63a] A. Xiong,[126] J. Xiong,[18a] D. Xu,[14] H. Xu,[63a] L. Xu,[63a] R. Xu,[131] T. Xu,[108] Y. Xu,[142] Z. Xu,[53] Z. Xu,[114a] B. Yabsley,[151] S. Yacoob,[34a] Y. Yamaguchi,[85] E. Yamashita,[157] H. Yamauchi,[160] T. Yamazaki,[18a] Y. Yamazaki,[86] S. Yan,[60] Z. Yan,[105] H. J. Yang,[63c,63d] H. T. Yang,[63a] S. Yang,[63a] T. Yang,[65c] X. Yang,[37] X. Yang,[14] Y. Yang,[46] Y. Yang,[63a] W-M. Yao,[18a] H. Ye,[56] J. Ye,[14] S. Ye,[30] X. Ye,[63a] Y. Yeh,[98] I. Yeletskikh,[40] B. Yeo,[18b] M. R. Yexley,[98] T. P. Yildirim,[129] P. Yin,[43] K. Yorita,[172] S. Younas,[28b] C. J. S. Young,[37] C. Young,[147] N. D. Young,[126] Y. Yu,[63a] J. Yuan,[14,114c] M. Yuan,[108] R. Yuan,[63d,63c] L. Yue,[98] M. Zaazoua,[63a] B. Zabinski,[88] I. Zahir,[36a] Z. K. Zak,[88] T. Zakareishvili,[167] S. Zambito,[57] J. A. Zamora Saa,[140d,140b] J. Zang,[157] D. Zanzi,[55] R. Zanzottera,[72a,72b] O. Zaplatilek,[135] C. Zeitnitz,[175] H. Zeng,[14] J. C. Zeng,[166] D. T. Zenger Jr.,[27] O. Zenin,[39] T. Ženiš,[29a] S. Zenz,[96] S. Zerradi,[36a] D. Zerwas,[67] M. Zhai,[14,114c] D. F. Zhang,[143] J. Zhang,[63b] J. Zhang,[6] K. Zhang,[14,114c] L. Zhang,[63a] L. Zhang,[114a] P. Zhang,[14,114c] R. Zhang,[174] S. Zhang,[91] T. Zhang,[157] X. Zhang,[63c] Y. Zhang,[142] Y. Zhang,[98] Y. Zhang,[63a] Y. Zhang,[114a] Z. Zhang,[18a] Z. Zhang,[63b] Z. Zhang,[67] H. Zhao,[142] T. Zhao,[63b] Y. Zhao,[35] Z. Zhao,[63a]

Z. Zhao,[63a] A. Zhemchugov,[40] J. Zheng,[114a] K. Zheng,[166] X. Zheng,[63a] Z. Zheng,[147] D. Zhong,[166] B. Zhou,[108] H. Zhou,[7] N. Zhou,[63c] Y. Zhou,[15] Y. Zhou,[114a] Y. Zhou,[7] C. G. Zhu,[63b] J. Zhu,[108] X. Zhu,[63d] Y. Zhu,[63c] Y. Zhu,[63a] X. Zhuang,[14] K. Zhukov,[69] N. I. Zimine,[40] J. Zinsser,[64b] M. Ziolkowski,[145] L. Živković,[16] A. Zoccoli,[24b,24a] K. Zoch,[62] T. G. Zorbas,[143] O. Zormpa,[47] W. Zou,[43] and L. Zwalinski[37]

(ATLAS Collaboration)

[1]*Department of Physics, University of Adelaide, Adelaide, Australia*
[2]*Department of Physics, University of Alberta, Edmonton, Alberta, Canada*
[3a]*Department of Physics, Ankara University, Ankara, Türkiye*
[3b]*Division of Physics, TOBB University of Economics and Technology, Ankara, Türkiye*
[4]*LAPP, Université Savoie Mont Blanc, CNRS/IN2P3, Annecy, France*
[5]*APC, Université Paris Cité, CNRS/IN2P3, Paris, France*
[6]*High Energy Physics Division, Argonne National Laboratory, Argonne, Illinois, USA*
[7]*Department of Physics, University of Arizona, Tucson, Arizona, USA*
[8]*Department of Physics, University of Texas at Arlington, Arlington, Texas, USA*
[9]*Physics Department, National and Kapodistrian University of Athens, Athens, Greece*
[10]*Physics Department, National Technical University of Athens, Zografou, Greece*
[11]*Department of Physics, University of Texas at Austin, Austin, Texas, USA*
[12]*Institute of Physics, Azerbaijan Academy of Sciences, Baku, Azerbaijan*
[13]*Institut de Física d'Altes Energies (IFAE), Barcelona Institute of Science and Technology, Barcelona, Spain*
[14]*Institute of High Energy Physics, Chinese Academy of Sciences, Beijing, China*
[15]*Physics Department, Tsinghua University, Beijing, China*
[16]*Institute of Physics, University of Belgrade, Belgrade, Serbia*
[17]*Department for Physics and Technology, University of Bergen, Bergen, Norway*
[18a]*Physics Division, Lawrence Berkeley National Laboratory, Berkeley, California, USA*
[18b]*University of California, Berkeley, California, USA*
[19]*Institut für Physik, Humboldt Universität zu Berlin, Berlin, Germany*
[20]*Albert Einstein Center for Fundamental Physics and Laboratory for High Energy Physics, University of Bern, Bern, Switzerland*
[21]*School of Physics and Astronomy, University of Birmingham, Birmingham, United Kingdom*
[22a]*Department of Physics, Bogazici University, Istanbul, Türkiye*
[22b]*Department of Physics Engineering, Gaziantep University, Gaziantep, Türkiye*
[22c]*Department of Physics, Istanbul University, Istanbul, Türkiye*
[23a]*Facultad de Ciencias y Centro de Investigaciónes, Universidad Antonio Nariño, Bogotá, Colombia*
[23b]*Departamento de Física, Universidad Nacional de Colombia, Bogotá, Colombia*
[24a]*Dipartimento di Fisica e Astronomia A. Righi, Università di Bologna, Bologna, Italy*
[24b]*INFN Sezione di Bologna, Bologna, Italy*
[25]*Physikalisches Institut, Universität Bonn, Bonn, Germany*
[26]*Department of Physics, Boston University, Boston, Massachusetts, USA*
[27]*Department of Physics, Brandeis University, Waltham, Massachusetts, USA*
[28a]*Transilvania University of Brasov, Brasov, Romania*
[28b]*Horia Hulubei National Institute of Physics and Nuclear Engineering, Bucharest, Romania*
[28c]*Department of Physics, Alexandru Ioan Cuza University of Iasi, Iasi, Romania*
[28d]*National Institute for Research and Development of Isotopic and Molecular Technologies, Physics Department, Cluj-Napoca, Romania*
[28e]*National University of Science and Technology Politechnica, Bucharest, Romania*
[28f]*West University in Timisoara, Timisoara, Romania*
[28g]*Faculty of Physics, University of Bucharest, Bucharest, Romania*
[29a]*Faculty of Mathematics, Physics and Informatics, Comenius University, Bratislava, Slovak Republic*
[29b]*Department of Subnuclear Physics, Institute of Experimental Physics of the Slovak Academy of Sciences, Kosice, Slovak Republic*
[30]*Physics Department, Brookhaven National Laboratory, Upton, New York, USA*
[31]*Universidad de Buenos Aires, Facultad de Ciencias Exactas y Naturales, Departamento de Física, y CONICET, Instituto de Física de Buenos Aires (IFIBA), Buenos Aires, Argentina*
[32]*California State University, California, USA*
[33]*Cavendish Laboratory, University of Cambridge, Cambridge, United Kingdom*
[34a]*Department of Physics, University of Cape Town, Cape Town, South Africa*

[34b]iThemba Labs, Western Cape, South Africa
[34c]Department of Mechanical Engineering Science, University of Johannesburg, Johannesburg, South Africa
[34d]National Institute of Physics, University of the Philippines Diliman (Philippines), Quezon City, Philippines
[34e]University of South Africa, Department of Physics, Pretoria, South Africa
[34f]University of Zululand, KwaDlangezwa, South Africa
[34g]School of Physics, University of the Witwatersrand, Johannesburg, South Africa
[35]Department of Physics, Carleton University, Ottawa, Ontario, Canada
[36a]Faculté des Sciences Ain Chock, Université Hassan II de Casablanca, Casablanca, Morocco
[36b]Faculté des Sciences, Université Ibn-Tofail, Kénitra, Morocco
[36c]Faculté des Sciences Semlalia, Université Cadi Ayyad, LPHEA-Marrakech, Morocco
[36d]LPMR, Faculté des Sciences, Université Mohamed Premier, Oujda, Morocco
[36e]Faculté des sciences, Université Mohammed V, Rabat, Morocco
[36f]Institute of Applied Physics, Mohammed VI Polytechnic University, Ben Guerir, Morocco
[37]CERN, Geneva, Switzerland
[38]Affiliated with an institute formerly covered by a cooperation agreement with CERN
[39]Affiliated with an institute covered by a cooperation agreement with CERN
[40]Affiliated with an international laboratory covered by a cooperation agreement with CERN
[41]Enrico Fermi Institute, University of Chicago, Chicago, Illinois, USA
[42]LPC, Université Clermont Auvergne, CNRS/IN2P3, Clermont-Ferrand, France
[43]Nevis Laboratory, Columbia University, Irvington, New York, USA
[44]Niels Bohr Institute, University of Copenhagen, Copenhagen, Denmark
[45a]Dipartimento di Fisica, Università della Calabria, Rende, Italy
[45b]INFN Gruppo Collegato di Cosenza, Laboratori Nazionali di Frascati, Italy
[46]Physics Department, Southern Methodist University, Dallas, Texas, USA
[47]National Centre for Scientific Research "Demokritos", Agia Paraskevi, Greece
[48a]Department of Physics, Stockholm University, Stockholm, Sweden
[48b]Oskar Klein Centre, Stockholm, Sweden
[49]Deutsches Elektronen-Synchrotron DESY, Hamburg and Zeuthen, Germany
[50]Fakultät Physik, Technische Universität Dortmund, Dortmund, Germany
[51]Institut für Kern- und Teilchenphysik, Technische Universität Dresden, Dresden, Germany
[52]Department of Physics, Duke University, Durham, North Carolina, USA
[53]SUPA—School of Physics and Astronomy, University of Edinburgh, Edinburgh, United Kingdom
[54]INFN e Laboratori Nazionali di Frascati, Frascati, Italy
[55]Physikalisches Institut, Albert-Ludwigs-Universität Freiburg, Freiburg, Germany
[56]II. Physikalisches Institut, Georg-August-Universität Göttingen, Göttingen, Germany
[57]Département de Physique Nucléaire et Corpusculaire, Université de Genève, Genève, Switzerland
[58a]Dipartimento di Fisica, Università di Genova, Genova, Italy
[58b]INFN Sezione di Genova, Genova, Italy
[59]II. Physikalisches Institut, Justus-Liebig-Universität Giessen, Giessen, Germany
[60]SUPA—School of Physics and Astronomy, University of Glasgow, Glasgow, United Kingdom
[61]LPSC, Université Grenoble Alpes, CNRS/IN2P3, Grenoble INP, Grenoble, France
[62]Laboratory for Particle Physics and Cosmology, Harvard University, Cambridge, Massachusetts, USA
[63a]Department of Modern Physics and State Key Laboratory of Particle Detection and Electronics, University of Science and Technology of China, Hefei, China
[63b]Institute of Frontier and Interdisciplinary Science and Key Laboratory of Particle Physics and Particle Irradiation (MOE), Shandong University, Qingdao, China
[63c]School of Physics and Astronomy, Shanghai Jiao Tong University, Key Laboratory for Particle Astrophysics and Cosmology (MOE), SKLPPC, Shanghai, China
[63d]Tsung-Dao Lee Institute, Shanghai, China
[63e]School of Physics, Zhengzhou University, Zhengzhou, China
[64a]Kirchhoff-Institut für Physik, Ruprecht-Karls-Universität Heidelberg, Heidelberg, Germany
[64b]Physikalisches Institut, Ruprecht-Karls-Universität Heidelberg, Heidelberg, Germany
[65a]Department of Physics, Chinese University of Hong Kong, Shatin, N.T., Hong Kong, China
[65b]Department of Physics, University of Hong Kong, Hong Kong, China
[65c]Department of Physics and Institute for Advanced Study, Hong Kong University of Science and Technology, Clear Water Bay, Kowloon, Hong Kong, China
[66]Department of Physics, National Tsing Hua University, Hsinchu, Taiwan
[67]IJCLab, Université Paris-Saclay, CNRS/IN2P3, 91405, Orsay, France

[68]*Centro Nacional de Microelectrónica (IMB-CNM-CSIC), Barcelona, Spain*
[69]*Department of Physics, Indiana University, Bloomington, Indiana, USA*
[70a]*INFN Gruppo Collegato di Udine, Sezione di Trieste, Udine, Italy*
[70b]*ICTP, Trieste, Italy*
[70c]*Dipartimento Politecnico di Ingegneria e Architettura, Università di Udine, Udine, Italy*
[71a]*INFN Sezione di Lecce, Lecce, Italy*
[71b]*Dipartimento di Matematica e Fisica, Università del Salento, Lecce, Italy*
[72a]*INFN Sezione di Milano, Milano, Italy*
[72b]*Dipartimento di Fisica, Università di Milano, Milano, Italy*
[73a]*INFN Sezione di Napoli, Napoli, Italy*
[73b]*Dipartimento di Fisica, Università di Napoli, Napoli, Italy*
[74a]*INFN Sezione di Pavia, Pavia, Italy*
[74b]*Dipartimento di Fisica, Università di Pavia, Pavia, Italy*
[75a]*INFN Sezione di Pisa, Pisa, Italy*
[75b]*Dipartimento di Fisica E. Fermi, Università di Pisa, Pisa, Italy*
[76a]*INFN Sezione di Roma, Roma, Italy*
[76b]*Dipartimento di Fisica, Sapienza Università di Roma, Roma, Italy*
[77a]*INFN Sezione di Roma Tor Vergata, Roma, Italy*
[77b]*Dipartimento di Fisica, Università di Roma Tor Vergata, Roma, Italy*
[78a]*INFN Sezione di Roma Tre, Roma, Italy*
[78b]*Dipartimento di Matematica e Fisica, Università Roma Tre, Roma, Italy*
[79a]*INFN-TIFPA, Italy*
[79b]*Università degli Studi di Trento, Trento, Italy*
[80]*Universität Innsbruck, Department of Astro and Particle Physics, Innsbruck, Austria*
[81]*University of Iowa, Iowa City, Iowa, USA*
[82]*Department of Physics and Astronomy, Iowa State University, Ames, Iowa, USA*
[83]*Istinye University, Sariyer, Istanbul, Türkiye*
[84a]*Departamento de Engenharia Elétrica, Universidade Federal de Juiz de Fora (UFJF), Juiz de Fora, Brazil*
[84b]*Universidade Federal do Rio De Janeiro COPPE/EE/IF, Rio de Janeiro, Brazil*
[84c]*Instituto de Física, Universidade de São Paulo, São Paulo, Brazil*
[84d]*Rio de Janeiro State University, Rio de Janeiro, Brazil*
[84e]*Federal University of Bahia, Bahia, Brazil*
[85]*KEK, High Energy Accelerator Research Organization, Tsukuba, Japan*
[86]*Graduate School of Science, Kobe University, Kobe, Japan*
[87a]*AGH University of Krakow, Faculty of Physics and Applied Computer Science, Krakow, Poland*
[87b]*Marian Smoluchowski Institute of Physics, Jagiellonian University, Krakow, Poland*
[88]*Institute of Nuclear Physics Polish Academy of Sciences, Krakow, Poland*
[89]*Faculty of Science, Kyoto University, Kyoto, Japan*
[90]*Research Center for Advanced Particle Physics and Department of Physics, Kyushu University, Fukuoka, Japan*
[91]*L2IT, Université de Toulouse, CNRS/IN2P3, UPS, Toulouse, France*
[92]*Instituto de Física La Plata, Universidad Nacional de La Plata and CONICET, La Plata, Argentina*
[93]*Physics Department, Lancaster University, Lancaster, United Kingdom*
[94]*Oliver Lodge Laboratory, University of Liverpool, Liverpool, United Kingdom*
[95]*Department of Experimental Particle Physics, Jožef Stefan Institute and Department of Physics, University of Ljubljana, Ljubljana, Slovenia*
[96]*School of Physics and Astronomy, Queen Mary University of London, London, United Kingdom*
[97]*Department of Physics, Royal Holloway University of London, Egham, United Kingdom*
[98]*Department of Physics and Astronomy, University College London, London, United Kingdom*
[99]*Louisiana Tech University, Ruston, Louisiana, USA*
[100]*Fysiska institutionen, Lunds universitet, Lund, Sweden*
[101]*Departamento de Física Teorica C-15 and CIAFF, Universidad Autónoma de Madrid, Madrid, Spain*
[102]*Institut für Physik, Universität Mainz, Mainz, Germany*
[103]*School of Physics and Astronomy, University of Manchester, Manchester, United Kingdom*
[104]*CPPM, Aix-Marseille Université, CNRS/IN2P3, Marseille, France*
[105]*Department of Physics, University of Massachusetts, Amherst, Massachusetts, USA*
[106]*Department of Physics, McGill University, Montreal, Quebec, Canada*
[107]*School of Physics, University of Melbourne, Victoria, Australia*
[108]*Department of Physics, University of Michigan, Ann Arbor, Michigan, USA*

[109]Department of Physics and Astronomy, Michigan State University, East Lansing, Michigan, USA
[110]Group of Particle Physics, University of Montreal, Montreal, Quebec, Canada
[111]Fakultät für Physik, Ludwig-Maximilians-Universität München, München, Germany
[112]Max-Planck-Institut für Physik (Werner-Heisenberg-Institut), München, Germany
[113]Graduate School of Science and Kobayashi-Maskawa Institute, Nagoya University, Nagoya, Japan
[114a]Department of Physics, Nanjing University, Nanjing, China
[114b]School of Science, Shenzhen Campus of Sun Yat-sen University, China
[114c]University of Chinese Academy of Science (UCAS), Beijing, China
[115]Department of Physics and Astronomy, University of New Mexico, Albuquerque, New Mexico, USA
[116]Institute for Mathematics, Astrophysics and Particle Physics, Radboud University/Nikhef, Nijmegen, Netherlands
[117]Nikhef National Institute for Subatomic Physics and University of Amsterdam, Amsterdam, Netherlands
[118]Department of Physics, Northern Illinois University, DeKalb, Illinois, USA
[119a]New York University Abu Dhabi, Abu Dhabi, United Arab Emirates
[119b]United Arab Emirates University, Al Ain, United Arab Emirates
[120]Department of Physics, New York University, New York, New York, USA
[121]Ochanomizu University, Otsuka, Bunkyo-ku, Tokyo, Japan
[122]Ohio State University, Columbus, Ohio, USA
[123]Homer L. Dodge Department of Physics and Astronomy, University of Oklahoma, Norman, Oklahoma, USA
[124]Department of Physics, Oklahoma State University, Stillwater, Oklahoma, USA
[125]Palacký University, Joint Laboratory of Optics, Olomouc, Czech Republic
[126]Institute for Fundamental Science, University of Oregon, Eugene, Oregon, USA
[127]Graduate School of Science, Osaka University, Osaka, Japan
[128]Department of Physics, University of Oslo, Oslo, Norway
[129]Department of Physics, Oxford University, Oxford, United Kingdom
[130]LPNHE, Sorbonne Université, Université Paris Cité, CNRS/IN2P3, Paris, France
[131]Department of Physics, University of Pennsylvania, Philadelphia, Pennsylvania, USA
[132]Department of Physics and Astronomy, University of Pittsburgh, Pittsburgh, Pennsylvania, USA
[133a]Laboratório de Instrumentação e Física Experimental de Partículas—LIP, Lisboa, Portugal
[133b]Departamento de Física, Faculdade de Ciências, Universidade de Lisboa, Lisboa, Portugal
[133c]Departamento de Física, Universidade de Coimbra, Coimbra, Portugal
[133d]Centro de Física Nuclear da Universidade de Lisboa, Lisboa, Portugal
[133e]Departamento de Física, Escola de Ciências, Universidade do Minho, Braga, Portugal
[133f]Departamento de Física Teórica y del Cosmos, Universidad de Granada, Granada, Spain
[133g]Departamento de Física, Instituto Superior Técnico, Universidade de Lisboa, Lisboa, Portugal
[134]Institute of Physics of the Czech Academy of Sciences, Prague, Czech Republic
[135]Czech Technical University in Prague, Prague, Czech Republic
[136]Charles University, Faculty of Mathematics and Physics, Prague, Czech Republic
[137]Particle Physics Department, Rutherford Appleton Laboratory, Didcot, United Kingdom
[138]IRFU, CEA, Université Paris-Saclay, Gif-sur-Yvette, France
[139]Santa Cruz Institute for Particle Physics, University of California Santa Cruz, Santa Cruz, California, USA
[140a]Departamento de Física, Pontificia Universidad Católica de Chile, Santiago, Chile
[140b]Millennium Institute for Subatomic Physics at High Energy Frontier (SAPHIR), Santiago, Chile
[140c]Instituto de Investigación Multidisciplinario en Ciencia y Tecnología, y Departamento de Física, Universidad de La Serena, La Serena, Chile
[140d]Universidad Andres Bello, Department of Physics, Santiago, Chile
[140e]Instituto de Alta Investigación, Universidad de Tarapacá, Arica, Chile
[140f]Departamento de Física, Universidad Técnica Federico Santa María, Valparaíso, Chile
[141]Department of Physics, Institute of Science, Tokyo, Japan
[142]Department of Physics, University of Washington, Seattle, Washington, USA
[143]Department of Physics and Astronomy, University of Sheffield, Sheffield, United Kingdom
[144]Department of Physics, Shinshu University, Nagano, Japan
[145]Department Physik, Universität Siegen, Siegen, Germany
[146]Department of Physics, Simon Fraser University, Burnaby, British Columbia, Canada
[147]SLAC National Accelerator Laboratory, Stanford, California, USA
[148]Department of Physics, Royal Institute of Technology, Stockholm, Sweden
[149]Departments of Physics and Astronomy, Stony Brook University, Stony Brook, New York, USA
[150]Department of Physics and Astronomy, University of Sussex, Brighton, United Kingdom

[151]*School of Physics, University of Sydney, Sydney, Australia*
[152]*Institute of Physics, Academia Sinica, Taipei, Taiwan*
[153a]*E. Andronikashvili Institute of Physics, Iv. Javakhishvili Tbilisi State University, Tbilisi, Georgia*
[153b]*High Energy Physics Institute, Tbilisi State University, Tbilisi, Georgia*
[153c]*University of Georgia, Tbilisi, Georgia*
[154]*Department of Physics, Technion, Israel Institute of Technology, Haifa, Israel*
[155]*Raymond and Beverly Sackler School of Physics and Astronomy, Tel Aviv University, Tel Aviv, Israel*
[156]*Department of Physics, Aristotle University of Thessaloniki, Thessaloniki, Greece*
[157]*International Center for Elementary Particle Physics and Department of Physics, University of Tokyo, Tokyo, Japan*
[158]*Department of Physics, University of Toronto, Toronto, Ontario, Canada*
[159a]*TRIUMF, Vancouver, British Columbia, Canada*
[159b]*Department of Physics and Astronomy, York University, Toronto, Ontario, Canada*
[160]*Division of Physics and Tomonaga Center for the History of the Universe, Faculty of Pure and Applied Sciences, University of Tsukuba, Tsukuba, Japan*
[161]*Department of Physics and Astronomy, Tufts University, Medford, Massachusetts, USA*
[162]*Department of Physics and Astronomy, University of California Irvine, Irvine, California, USA*
[163]*University of West Attica, Athens, Greece*
[164]*University of Sharjah, Sharjah, United Arab Emirates*
[165]*Department of Physics and Astronomy, University of Uppsala, Uppsala, Sweden*
[166]*Department of Physics, University of Illinois, Urbana, Illinois, USA*
[167]*Instituto de Física Corpuscular (IFIC), Centro Mixto Universidad de Valencia—CSIC, Valencia, Spain*
[168]*Department of Physics, University of British Columbia, Vancouver, British Columbia, Canada*
[169]*Department of Physics and Astronomy, University of Victoria, Victoria, British Columbia, Canada*
[170]*Fakultät für Physik und Astronomie, Julius-Maximilians-Universität Würzburg, Würzburg, Germany*
[171]*Department of Physics, University of Warwick, Coventry, United Kingdom*
[172]*Waseda University, Tokyo, Japan*
[173]*Department of Particle Physics and Astrophysics, Weizmann Institute of Science, Rehovot, Israel*
[174]*Department of Physics, University of Wisconsin, Madison, Wisconsin, USA*
[175]*Fakultät für Mathematik und Naturwissenschaften, Fachgruppe Physik, Bergische Universität Wuppertal, Wuppertal, Germany*
[176]*Department of Physics, Yale University, New Haven, Connecticut, USA*
[177]*Yerevan Physics Institute, Yerevan, Armenia*

[a]Deceased.
[b]Also at Department of Physics, King's College London, London, United Kingdom.
[c]Also at Institute of Physics, Azerbaijan Academy of Sciences, Baku, Azerbaijan.
[d]Also at Imam Mohammad Ibn Saud Islamic University, Saudi Arabia.
[e]Also at TRIUMF, Vancouver, British Columbia, Canada.
[f]Also at Department of Physics, University of Thessaly, Greece.
[g]Also at An-Najah National University, Nablus, Palestine.
[h]Also at Department of Physics, University of Fribourg, Fribourg, Switzerland.
[i]Also at Department of Physics, Westmont College, Santa Barbara, USA.
[j]Also at Departament de Fisica de la Universitat Autonoma de Barcelona, Barcelona, Spain.
[k]Also at Affiliated with an institute covered by a cooperation agreement with CERN.
[l]Also at The Collaborative Innovation Center of Quantum Matter (CICQM), Beijing, China.
[m]Also at Faculty of Physics, Sofia University, 'St. Kliment Ohridski', Sofia, Bulgaria.
[n]Also at Università di Napoli Parthenope, Napoli, Italy.
[o]Also at Institute of Particle Physics (IPP), Canada.
[p]Also at Department of Physics, Bolu Abant Izzet Baysal University, Bolu, Türkiye.
[q]Also at Borough of Manhattan Community College, City University of New York, New York, New York, USA.
[r]Also at National Institute of Physics, University of the Philippines Diliman (Philippines), Philippines.
[s]Also at Department of Financial and Management Engineering, University of the Aegean, Chios, Greece.
[t]Also at Institucio Catalana de Recerca i Estudis Avancats, ICREA, Barcelona, Spain.
[u]Also at Henan University, China.
[v]Also at Technical University of Munich, Munich, Germany.
[w]Also at CMD-AC UNEC Research Center, Azerbaijan State University of Economics (UNEC), Azerbaijan.
[x]Also at Yeditepe University, Physics Department, Istanbul, Türkiye.
[y]Also at CERN, Geneva, Switzerland.
[z]Also at Center for Interdisciplinary Research and Innovation (CIRI-AUTH), Thessaloniki, Greece.

[aa]Also at University of the Western Cape, South Africa.
[bb]Also at Hellenic Open University, Patras, Greece.
[cc]Also at Center for High Energy Physics, Peking University, China.
[dd]Also at Department of Mathematical Sciences, University of South Africa, Johannesburg, South Africa.
[ee]Also at Department of Physics, Stellenbosch University, South Africa.
[ff]Also at Department of Physics, California State University, Sacramento, USA.
[gg]Also at University of Colorado Boulder, Department of Physics, Colorado, USA.
[hh]Also at Département de Physique Nucléaire et Corpusculaire, Université de Genève, Genève, Switzerland.
[ii]Also at Institut für Experimentalphysik, Universität Hamburg, Hamburg, Germany.
[jj]Also at Institute for Nuclear Research and Nuclear Energy (INRNE) of the Bulgarian Academy of Sciences, Sofia, Bulgaria.
[kk]Also at Washington College, Chestertown, Maryland, USA.
[ll]Also at Institute of Applied Physics, Mohammed VI Polytechnic University, Ben Guerir, Morocco.
[mm]Also at Department of Physics, Stanford University, Stanford California, USA.
[nn]Also at Institute of Physics and Technology, Mongolian Academy of Sciences, Ulaanbaatar, Mongolia.